Table 1 List of primers used for RT-PCR.

Gene name	Species	(5′) Sense primers (3′)	(5′)Antisense primers (3′)
GAPDH	Ms	ACCACAGTCCATGCCATCAC	TCCACCACCCTGTTGCTGTA
HoxB4	Hs	AGAGGCGAGAGAGCAGCTT	TTCCTTCTCCAGCTCCAAGA
Oct-3/4	Ms	GTTTGCCAAGCTGCTGAAGC	TCTAGCCCAAGCTGATTGGC
GFP	–	CACATGAAGCAGCACGACTT	TGCTCAGGTAGTGGTTGTCG
Flk-1	Ms	TCTGTGGTTCTGCGTGGAGA	GTATCATTTCCAACCACCC
Gata1	Ms	TTGTGAGGCCAGAGAGTGTG	TTCCTCGTCTGGATTCCATC
Gata1 (real-time PCR)	Ms	GTCAGAACCGGCCTCTCATC	GTGGTCGTTTGACAGTTAGTGCAT
Tel	Ms	CTGAAGCAGAGGAAATCTCGAATG	GGCAGGCAGTGATTATTCTCGA
c-myb	Ms	CCTCACCTCCATCTCAGCTC	GCTGGTGAGGCACTTTCTTC
β-H1	Ms	AGTCCCCATGGAGTCAAAGA	CTCAAGGAGACCTTTGCTCA
β-Major	Ms	CTGACAGATGCTCTCTTGGG	CACAACCCCAGAAACAGACA
CXCR4	Ms	GTCTATGTGGGCGTCTGGAT	GGCAGAGCTTTTGAACTTGG

(PBS/2%FBS). Dead cells were excluded from the analysis by 7-amino actinomycin D (7-AAD, eBioscience). Analysis was performed on an LSRFortessa flow cytometer by using FACS-Diva software (BD Bioscience). For detection of transgene expression by Ad vectors, EB-derived total cells or $CD41^+c\text{-}kit^+$ cells were transduced with Ad-DsRed or Ad-CA-GFP, respectively, for 1.5 h. At 48 h of incubation with the hematopoietic cytokines as described above, transgene expression in the cells was analyzed by flow cytometry.

Colony assay

A colony-forming assay was performed by plating ES cell-derived hematopoietic cells or iPS cell-derived hematopoietic cells into methylcellulose medium M3434 (Stem Cell Technologies, Vancouver, BC, Canada). After incubation at 37 °C and 5% CO_2 for 10 to 14 days in a humidified atmosphere, colony numbers were counted. The morphology of colonies was observed using an inverted light microscope.

RT-PCR

Total RNA was isolated with the use of ISOGENE (Nippon Gene, Tokyo, Japan). cDNA was synthesized by using Super-Script II reverse transcriptase (Invitrogen) and the oligo(dT) primer. Semi-quantitative PCR was performed with the use of TaKaRa ExTaq HS DNA polymerase (Takara, Shiga, Japan). The PCR conditions were 94 °C for 2 min, followed by the appropriate number of cycles of 94 °C for 15 s, 55 °C for 30 s with 72 °C for 30 s and a final extension of 72 °C for 1 min, except for the addition of 5% dimethyl sulfoxide in the case of hHoxB4 cDNA amplification. The product was assessed by 2% agarose gel electrophoresis followed by ethidium bromide staining. Quantitative real-time PCR was performed using StepOnePlus real-time PCR system with FAST SYBR Green Master Mix (Applied Biosystems, Foster-City, CA). The sequences of the primers used for in this study are listed in Table 1.

Supplementary materials related to this article can be found online at doi:10.1016/j.scr.2011.09.001.

Conflict of interest

The authors have no financial conflict of interest.

Acknowledgments

We thank Dr. S. Yamanaka for kindly providing the mouse iPS cell line 38C2 and 20D17. We would also like to thank Dr. J. Miyazaki and Dr. T. Imai for providing the CA promoter and anti-mouse CAR monoclonal antibody, respectively. We also thank Dr. K. Nishikawa (National Institute of Biomedical Innovation) for helpful comments. This work was supported by grants from the Ministry of Education, Culture, Sports, Science, and Technology (MEXT) of Japan and the Ministry of Health, Labour, and Welfare of Japan.

References

Arai, F., Hirao, A., Ohmura, M., Sato, H., Matsuoka, S., Takubo, K., Ito, K., Koh, G.Y., Suda, T., 2004. Tie2/angiopoietin-1 signaling regulates hematopoietic stem cell quiescence in the bone marrow niche. Cell 118, 149–161.

Bergelson, J.M., Cunningham, J.A., Droguett, G., Kurt-Jones, E.A., Krithivas, A., Hong, J.S., Horwitz, M.S., Crowell, R.L., Finberg, R.W., 1997. Isolation of a common receptor for Coxsackie B viruses and adenoviruses 2 and 5. Science 275, 1320–1323.

Bowles, K.M., Vallier, L., Smith, J.R., Alexander, M.R., Pedersen, R.A., 2006. HOXB4 overexpression promotes hematopoietic development by human embryonic stem cells. Stem Cells 24, 1359–1369.

Carson, S.D., 2000. Limited proteolysis of the coxsackievirus and adenovirus receptor (CAR) on HeLa cells exposed to trypsin. FEBS Lett. 484, 149–152.

Chadwick, K., Wang, L., Li, L., Menendez, P., Murdoch, B., Rouleau, A., Bhatia, M., 2003. Cytokines and BMP-4 promote hematopoietic differentiation of human embryonic stem cells. Blood 102, 906–915.

Evans, M.J., Kaufman, M.H., 1981. Establishment in culture of pluripotential cells from mouse embryos. Nature 292, 154–156.

Godin, I., Cumano, A., 2002. The hare and the tortoise: an embryonic haematopoietic race. Nat. Rev. Immunol. 2, 593–604.

Hacein-Bey-Abina, S., Von Kalle, C., Schmidt, M., McCormack, M.P., Wulffraat, N., Leboulch, P., Lim, A., Osborne, C.S., Pawliuk, R., Morillon, E., Sorensen, R., Forster, A., Fraser, P., Cohen, J.I., de Saint Basile, G., Alexander, I., Wintergerst, U., Frebourg, T., Aurias, A., Stoppa-Lyonnet, D., Romana, S., Radford-Weiss, I., Gross, F., Valensi, F., Delabesse, E., Macintyre, E., Sigaux, F., Soulier, J., Leiva, L.E., Wissler, M., Prinz, C., Rabbitts, T.H., Le Deist, F., Fischer, A., Cavazzana-Calvo, M., 2003. LMO2-associated clonal T cell proliferation in two patients after gene therapy for SCID-X1. Science 302, 415–419.

Inamura, M., Kawabata, K., Takayama, K., Tashiro, K., Sakurai, F., Katayama, K., Toyoda, M., Akutsu, H., Miyagawa, Y., Okita, H., Kiyokawa, N., Umezawa, A., Hayakawa, T., Furue, M.K., Mizuguchi, H., 2011. Efficient generation of hepatoblasts from human ES cells and iPS cells by transient overexpression of homeobox gene HEX. Mol. Ther. 19, 400–407.

Kawabata, K., Sakurai, F., Yamaguchi, T., Hayakawa, T., Mizuguchi, H., 2005. Efficient gene transfer into mouse embryonic stem cells with adenovirus vectors. Mol. Ther. 12, 547–554.

Keller, G., 2005. Embryonic stem cell differentiation: emergence of a new era in biology and medicine. Genes Dev. 19, 1129–1155.

Kim, K., Doi, A., Wen, B., Ng, K., Zhao, R., Cahan, P., Kim, J., Aryee, M.J., Ji, H., Ehrlich, L.I., Yabuuchi, A., Takeuchi, A., Cunniff, K.C., Hongguang, H., McKinney-Freeman, S., Naveiras, O., Yoon, T.J., Irizarry, R.A., Jung, N., Seita, J., Hanna, J., Murakami, P., Jaenisch, R., Weissleder, R., Orkin, S.H., Weissman, I.L., Feinberg, A.P., Daley, G.Q., 2010. Epigenetic memory in induced pluripotent stem cells. Nature 467, 285–290.

Kulkeaw, K., Horio, Y., Mizuochi, C., Ogawa, M., Sugiyama, D., 2010. Variation in hematopoietic potential of induced pluripotent stem cell lines. Stem Cell Rev. 6, 381–389.

Kurita, R., Sasaki, E., Yokoo, T., Hiroyama, T., Takasugi, K., Imoto, H., Izawa, K., Dong, Y., Hashiguchi, T., Soda, Y., Maeda, T., Suehiro, Y., Tanioka, Y., Nakazaki, Y., Tani, K., 2006. Tal1/Scl gene transduction using a lentiviral vector stimulates highly efficient hematopoietic cell differentiation from common marmoset (*Callithrix jacchus*) embryonic stem cells. Stem Cells 24, 2014–2022.

Kyba, M., Perlingeiro, R.C., Daley, G.Q., 2002. HoxB4 confers definitive lymphoid-myeloid engraftment potential on embryonic stem cell and yolk sac hematopoietic progenitors. Cell 109, 29–37.

Li, Z., Dullmann, J., Schiedlmeier, B., Schmidt, M., von Kalle, C., Meyer, J., Forster, M., Stocking, C., Wahlers, A., Frank, O., Ostertag, W., Kuhlcke, K., Eckert, H.G., Fehse, B., Baum, C., 2002. Murine leukemia induced by retroviral gene marking. Science 296, 497.

Maizel Jr., J.V., White, D.O. , Scharff, M.D., 1968. The polypeptides of adenovirus. I. Evidence for multiple protein components in the virion and a comparison of types 2, 7A, and 12. Virology 36, 115–125.

Matsumoto, K., Isagawa, T., Nishimura, T., Ogaeri, T., Eto, K., Miyazaki, S., Miyazaki, J., Aburatani, H., Nakauchi, H., Ema, H., 2009. Stepwise development of hematopoietic stem cells from embryonic stem cells. PLoS One 4, e4820.

McKinney-Freeman, S.L., Naveiras, O., Yates, F., Loewer, S., Philitas, M., Curran, M., Park, P.J., Daley, G.Q., 2009. Surface antigen phenotypes of hematopoietic stem cells from embryos and murine embryonic stem cells. Blood 114, 268–278.

Mikkola, H.K., Fujiwara, Y., Schlaeger, T.M., Traver, D., Orkin, S.H., 2003. Expression of CD41 marks the initiation of definitive hematopoiesis in the mouse embryo. Blood 101, 508–516.

Mitjavila-Garcia, M.T., Cailleret, M., Godin, I., Nogueira, M.M., Cohen-Solal, K., Schiavon, V., Lecluse, Y., Le Pesteur, F., Lagrue, A.H., Vainchenker, W., 2002. Expression of CD41 on hematopoietic progenitors derived from embryonic hematopoietic cells. Development 129, 2003–2013.

Mizuguchi, H., Kay, M.A., 1998. Efficient construction of a recombinant adenovirus vector by an improved in vitro ligation method. Hum. Gene Ther. 9, 2577–2583.

Mizuguchi, H., Kay, M.A., 1999. A simple method for constructing E1- and E1/E4-deleted recombinant adenoviral vectors. Hum. Gene Ther. 10, 2013–2017.

Nakano, T., Kodama, H., Honjo, T., 1994. Generation of lymphohematopoietic cells from embryonic stem cells in culture. Science 265, 1098–1101.

Niwa, H., Yamamura, K., Miyazaki, J., 1991. Efficient selection for high-expression transfectants with a novel eukaryotic vector. Gene 108, 193–199.

Okabe, M., Otsu, M., Ahn, D.H., Kobayashi, T., Morita, Y., Wakiyama, Y., Onodera, M., Eto, K., Ema, H., Nakauchi, H., 2009. Definitive proof for direct reprogramming of hematopoietic cells to pluripotency. Blood 114, 1764–1767.

Okita, K., Ichisaka, T., Yamanaka, S., 2007. Generation of germline-competent induced pluripotent stem cells. Nature 448, 313–317.

Pilat, S., Carotta, S., Schiedlmeier, B., Kamino, K., Mairhofer, A., Will, E., Modlich, U., Steinlein, P., Ostertag, W., Baum, C., Beug, H., Klump, H., 2005. HOXB4 enforces equivalent fates of ES-cell-derived and adult hematopoietic cells. Proc. Natl. Acad. Sci. U. S. A. 102, 12101–12106.

Polo, J.M., Liu, S., Figueroa, M.E., Kulalert, W., Eminli, S., Tan, K.Y., Apostolou, E., Stadtfeld, M., Li, Y., Shioda, T., Natesan, S., Wagers, A.J., Melnick, A., Evans, T., Hochedlinger, K., 2010. Cell type of origin influences the molecular and functional properties of mouse induced pluripotent stem cells. Nat. Biotechnol. 28, 848–855.

Schiedlmeier, B., Santos, A.C., Ribeiro, A., Moncaut, N., Lesinski, D., Auer, H., Kornacker, K., Ostertag, W., Baum, C., Mallo, M., Klump, H., 2007. HOXB4's road map to stem cell expansion. Proc. Natl. Acad. Sci. U. S. A. 104, 16952–16957.

Schmitt, T.M., de Pooter, R.F., Gronski, M.A., Cho, S.K., Ohashi, P.S., Zuniga-Pflucker, J.C., 2004. Induction of T cell development and establishment of T cell competence from embryonic stem cells differentiated in vitro. Nat. Immunol. 5, 410–417.

Takahashi, K., Yamanaka, S., 2006. Induction of pluripotent stem cells from mouse embryonic and adult fibroblast cultures by defined factors. Cell 126, 663–676.

Takahashi, K., Tanabe, K., Ohnuki, M., Narita, M., Ichisaka, T., Tomoda, K., Yamanaka, S., 2007. Induction of pluripotent stem cells from adult human fibroblasts by defined factors. Cell 131, 861–872.

Tashiro, K., Kawabata, K., Sakurai, H., Kurachi, S., Sakurai, F., Yamanishi, K., Mizuguchi, H., 2008. Efficient adenovirus vector-mediated PPAR gamma gene transfer into mouse embryoid bodies promotes adipocyte differentiation. J. Gene Med. 10, 498–507.

Tashiro, K., Inamura, M., Kawabata, K., Sakurai, F., Yamanishi, K., Hayakawa, T., Mizuguchi, H., 2009. Efficient adipocyte and osteoblast differentiation from mouse induced pluripotent stem cells by adenoviral transduction. Stem Cells 27, 1802–1811.

Tashiro, K., Kawabata, K., Inamura, M., Takayama, K., Furukawa, N., Sakurai, F., Katayama, K., Hayakawa, T., Furue, M.K., Mizuguchi, H., 2010. Adenovirus vector-mediated efficient transduction into human embryonic and induced pluripotent stem cells. Cell. Reprogram. 12, 501–507.

Thomson, J.A., Itskovitz-Eldor, J., Shapiro, S.S., Waknitz, M.A., Swiergiel, J.J., Marshall, V.S., Jones, J.M., 1998. Embryonic stem cell lines derived from human blastocysts. Science 282, 1145–1147.

Tomko, R.P., Xu, R., Philipson, L., 1997. HCAR and MCAR: the human and mouse cellular receptors for subgroup C adenoviruses and group B coxsackieviruses. Proc. Natl. Acad. Sci. U. S. A. 94, 3352–3356.

Vodyanik, M.A., Bork, J.A., Thomson, J.A., Slukvin, I.I., 2005. Human embryonic stem cell-derived CD34+ cells: efficient production in the coculture with OP9 stromal cells and analysis of lymphohematopoietic potential. Blood 105, 617–626.

Wang, Y., Yates, F., Naveiras, O., Ernst, P., Daley, G.Q., 2005. Embryonic stem cell-derived hematopoietic stem cells. Proc. Natl. Acad. Sci. U. S. A. 102, 19081–19086.

Williams, D., Baum, C., 2004. Gene therapy needs both trials and new strategies. Nature 429, 129.

Zhang, X.B., Beard, B.C., Trobridge, G.D., Wood, B.L., Sale, G.E., Sud, R., Humphries, R.K., Kiem, H.P., 2008. High incidence of leukemia in large animals after stem cell gene therapy with a HOXB4-expressing retroviral vector. J. Clin. Invest. 118, 1502–1510.

Efficient Generation of Functional Hepatocytes From Human Embryonic Stem Cells and Induced Pluripotent Stem Cells by HNF4α Transduction

Kazuo Takayama[1,2], Mitsuru Inamura[1,2], Kenji Kawabata[2,3], Kazufumi Katayama[1], Maiko Higuchi[2], Katsuhisa Tashiro[2], Aki Nonaka[2], Fuminori Sakurai[1], Takao Hayakawa[4,5], Miho Kusuda Furue[6,7] and Hiroyuki Mizuguchi[1,2,8]

[1]*Laboratory of Biochemistry and Molecular Biology, Graduate School of Pharmaceutical Sciences, Osaka University, Osaka, Japan;* [2]*Laboratory of Stem Cell Regulation, National Institute of Biomedical Innovation, Osaka, Japan;* [3]*Laboratory of Biomedical Innovation, Graduate School of Pharmaceutical Sciences, Osaka University, Osaka, Japan;* [4]*Pharmaceutics and Medical Devices Agency, Tokyo, Japan;* [5]*Pharmaceutical Research and Technology Institute, Kinki University, Osaka, Japan;* [6]*JCRB Cell Bank, Division of Bioresources, National Institute of Biomedical Innovation, Osaka, Japan;* [7]*Laboratory of Cell Processing, Institute for Frontier Medical Sciences, Kyoto University, Kyoto, Japan;* [8]*The Center for Advanced Medical Engineering and Informatics, Osaka University, Osaka, Japan*

Hepatocyte-like cells from human embryonic stem cells (ESCs) and induced pluripotent stem cells (iPSCs) are expected to be a useful source of cells drug discovery. Although we recently reported that hepatic commitment is promoted by transduction of SOX17 and HEX into human ESC- and iPSC-derived cells, these hepatocyte-like cells were not sufficiently mature for drug screening. To promote hepatic maturation, we utilized transduction of the hepatocyte nuclear factor 4α (HNF4α) gene, which is known as a master regulator of liver-specific gene expression. Adenovirus vector-mediated overexpression of HNF4α in hepatoblasts induced by SOX17 and HEX transduction led to upregulation of epithelial and mature hepatic markers such as cytochrome P450 (CYP) enzymes, and promoted hepatic maturation by activating the mesenchymal-to-epithelial transition (MET). Thus HNF4α might play an important role in the hepatic differentiation from human ESC-derived hepatoblasts by activating the MET. Furthermore, the hepatocyte like-cells could catalyze the toxication of several compounds. Our method would be a valuable tool for the efficient generation of functional hepatocytes derived from human ESCs and iPSCs, and the hepatocyte-like cells could be used for predicting drug toxicity.

Received 19 July 2011; accepted 28 September 2011; published online 8 November 2011. doi:10.1038/mt.2011.234

INTRODUCTION

Human embryonic stem cells (ESCs) and induced pluripotent stem cells (iPSCs) are able to replicate indefinitely and differentiate into most of the body's cell types.[1,2] They could provide an unlimited source of cells for various applications. Hepatocyte-like cells, which are differentiated from human ESCs and iPSCs, would be useful for basic research, regenerative medicine, and drug discovery.[3] In particular, it is expected that hepatocyte-like cells will be utilized as a tool for cytotoxicity screening in the early phase of pharmaceutical development. To catalyze the toxication of several compounds, hepatocyte-like cells need to be mature enough to exhibit hepatic functions, including high activity levels of the cytochrome P450 (CYP) enzymes. Because the present technology for the generation of hepatocyte-like cells from human ESCs and iPSCs, which is expected to be utilized for drug discovery, is not refined enough for this application, it is necessary to improve the efficiency of hepatic differentiation. Although conventional methods such as growth factor-mediated hepatic differentiation are useful to recapitulate liver development, they lead to only a heterogeneous hepatocyte population.[4–6] Recently, we showed that transcription factors are transiently transduced to promote hepatic differentiation in addition to the conventional differentiation method which uses only growth factors.[7] Ectopic expression of Sry-related HMG box 17 (SOX17) or hematopoietically expressed homeobox (HEX) by adenovirus (Ad) vectors in human ESC-derived mesendoderm or definitive endoderm (DE) cells markedly enhances the endoderm differentiation or hepatic commitment, respectively.[7,8] However, further hepatic maturation is required for drug screening.

The transcription factor hepatocyte nuclear factor 4α (HNF4α) is initially expressed in the developing hepatic diverticulum on E8.75,[9,10] and its expression is elevated as the liver develops. A previous loss-of-function study showed that HNF4α plays a critical role in liver development; conditional deletion of *HNF4α* in fetal hepatocytes results in the faint expression of many mature hepatic enzymes and the impairment of normal liver morphology.[11] The genome-scale chromatin immunoprecipitation assay showed that HNF4α binds to the promoters of nearly half of the genes expressed in the mouse liver,[12] including cell adhesion and junctional proteins,[13] which are important in

Correspondence: *Hiroyuki Mizuguchi, Laboratory of Biochemistry and Molecular Biology, Graduate School of Pharmaceutical Sciences, Osaka University, 1-6 Yamadaoka, Suita, Osaka 565-0871, Japan. E-mail: mizuguch@phs.osaka-u.ac.jp*

the hepatocyte epithelial structure.[14] In addition, HNF4α plays a critical role in hepatic differentiation and in a wide variety of liver functions, including lipid and glucose metabolism.[15,16] Although HNF4α could promote transdifferentiation into hepatic lineage from hematopoietic cells,[17] the function of HNF4α in hepatic differentiation from human ESCs and iPSCs remains unknown. A previous study showed that hepatic differentiation from mouse hepatic progenitor cells is promoted by HNF4α, although many of the hepatic markers that they examined were target genes of HNF4α.[18] They transplanted the HNF4α-overexpressed mouse hepatic progenitor cells to promote hepatic differentiation, but they did not examine the markers that relate to hepatic maturation such as CYP enzymes, conjugating enzymes, and hepatic transporters.

In this study, we examined the role of HNF4α in hepatic differentiation from human ESCs and iPSCs. The human ESC- and iPSC-derived hepatoblasts, which were efficiently generated by sequential transduction of SOX17 and HEX, were transduced with HNF4α-expressing Ad vector (Ad-HNF4α), and then the expression of hepatic markers of the hepatocyte-like cells were assessed. In addition, we examined whether or not the hepatocyte-like cells, which were generated by sequential transduction of SOX17, HEX, and HNF4α, were able to predict the toxicity of several compounds.

RESULTS

Stage-specific HNF4α transduction in hepatoblasts selectively promotes hepatic differentiation

The transcription factor HNF4α plays an important role in both liver generation[11] and hepatic differentiation from human ESCs and iPSCs (**Supplementary Figure S1**). We expected that hepatic differentiation could be accelerated by HNF4α transduction. To examine the effect of forced expression of HNF4α in the hepatic differentiation from human ESC- and iPSC-derived cells, we used a fiber-modified Ad vector.[19] Initially, we optimized the time period for Ad-HNF4α transduction. Human ESC (H9)-derived DE cells (day 6) (**Supplementary Figures S2** and **S3a**), hepatoblasts (day 9) (**Supplementary Figures S2** and **S3b**), or a heterogeneous population consisting of hepatoblasts, hepatocytes, and cholangiocytes (day 12) (**Supplementary Figures S2** and **S3c**) were transduced with Ad-HNF4α and then the Ad-HNF4α-transduced cells were cultured until day 20 of differentiation (**Figure 1**). We ascertained the expression of exogenous *HNF4α* in human ESC-derived hepatoblasts (day 9) transduced with Ad-HNF4α (**Supplementary Figure S4**). The transduction of Ad-HNF4α into human ESC-derived hepatoblasts (day 9) led to the highest expression levels of the hepatocyte markers *albumin* (*ALB*)[20] and *α-1-antitrypsin* (**Figure 1a**). In contrast, the expression levels of the cholangiocyte markers *cytokeratin 7* (*CK7*)[21] and *SOX9*[22] were

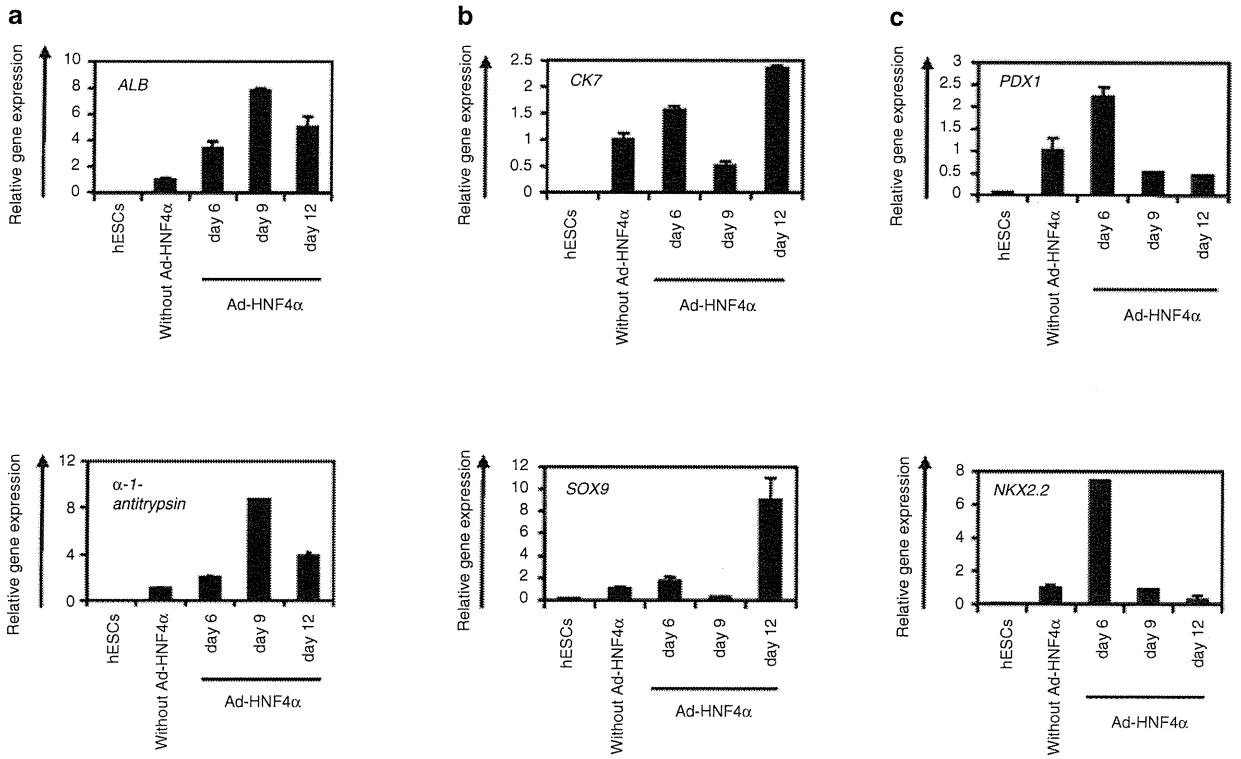

Figure 1 Transduction of HNF4α into hepatoblasts promotes hepatic differentiation. (**a–c**) The human ESC (H9)-derived cells, which were cultured for 6, 9, or 12 days according to the protocol described in **Figure 2a**, were transduced with 3,000 vector particles (VP)/cell of Ad-HNF4α for 1.5 hours and cultured until day 20. The gene expression levels of (**a**) hepatocyte markers (*ALB* and *α-1-antitrypsin*), (**b**) cholangiocyte markers (*CK7* and *SOX9*), and (**c**) pancreas markers (*PDX1* and *NKX2.2*) were examined by real-time RT-PCR on day 0 (human ESCs (hESCs)) or day 20 of differentiation. The horizontal axis represents the days when the cells were transduced with Ad-HNF4α. On the y-axis, the level of the cells without Ad-HNF4α transduction on day 20 was taken as 1.0. All data are represented as means ± SD (n = 3). ESC, embryonic stem cell; HNF4α, hepatocyte nuclear factor 4α; RT-PCR, reverse transcription-PCR.

downregulated in the cells transduced on day 9 as compared with nontransduced cells (**Figure 1b**). This might be because hepatic differentiation was selectively promoted and biliary differentiation was repressed by the transduction of HNF4α in hepatoblasts. The expression levels of the pancreas markers *PDX1*[23] and *NKX2.2*[24] did not make any change in the cells transduced on day 9 as compared with nontransduced cells (**Figure 1c**). Interestingly, the expression levels of the pancreas markers were upregulated, when Ad-HNF4α transduction was performed into DE cells (day 6) (**Figure 1c**). These results suggest that HNF4α might promote not only hepatic differentiation but also pancreatic differentiation, although the optimal stage of HNF4 transduction for the differentiation of each cell is different. We have confirmed that there was no difference between nontransduced cells and Ad-LacZ-transduced cells in the gene expression levels of all the markers investigated in **Figure 1a–c** (data not shown). We also confirmed that Ad vector-mediated gene expression in the human ESC-derived hepatoblasts (day 9) continued until day 14 and almost disappeared on day 18 (**Supplementary Figure S5**). These results indicated that the stage-specific HNF4α overexpression in human ESC-derived hepatoblasts (day 9) was essential for promoting efficient hepatic differentiation.

Transduction of HNF4α into human ESC- and iPSC-derived hepatoblasts efficiently promotes hepatic maturation

From the results of **Figure 1**, we decided to transduce hepatoblasts (day 9) with Ad-HNF4α. To determine whether hepatic maturation is promoted by Ad-HNF4α transduction, Ad-HNF4α-transduced cells were cultured until day 20 of differentiation according to the schematic protocol described in **Figure 2a**. After the hepatic maturation, the morphology of human ESCs was gradually changed into that of hepatocytes: polygonal with distinct round nuclei (day 20) (**Figure 2b**). Interestingly, a portion of the hepatocyte-like cells, which were ALB[20]-, CK18[21]-, CYP2D6-, and CYP3A4[25]-positive cells, had double nuclei, which was also observed in primary human hepatocytes (**Figure 2b,c**, and **Supplementary Figure S6**). We also examined the hepatic gene expression levels on day 20 of differentiation (**Figure 3a,b**). The gene expression analysis of *CYP1A2*, *CYP2C9*, *CYP2C19*, *CYP2D6*, *CYP3A4*, and *CYP7A1*[25] showed higher expression levels in all of Ad-SOX17-, Ad-HEX-, and Ad-HNF4α-transduced cells (three factors-transduced cells) as compared with those in both Ad-SOX17- and Ad-HEX-transduced cells (two factors-transduced cells) on day 20 (**Figure 3a**). The gene expression level of NADPH-CYP reductase

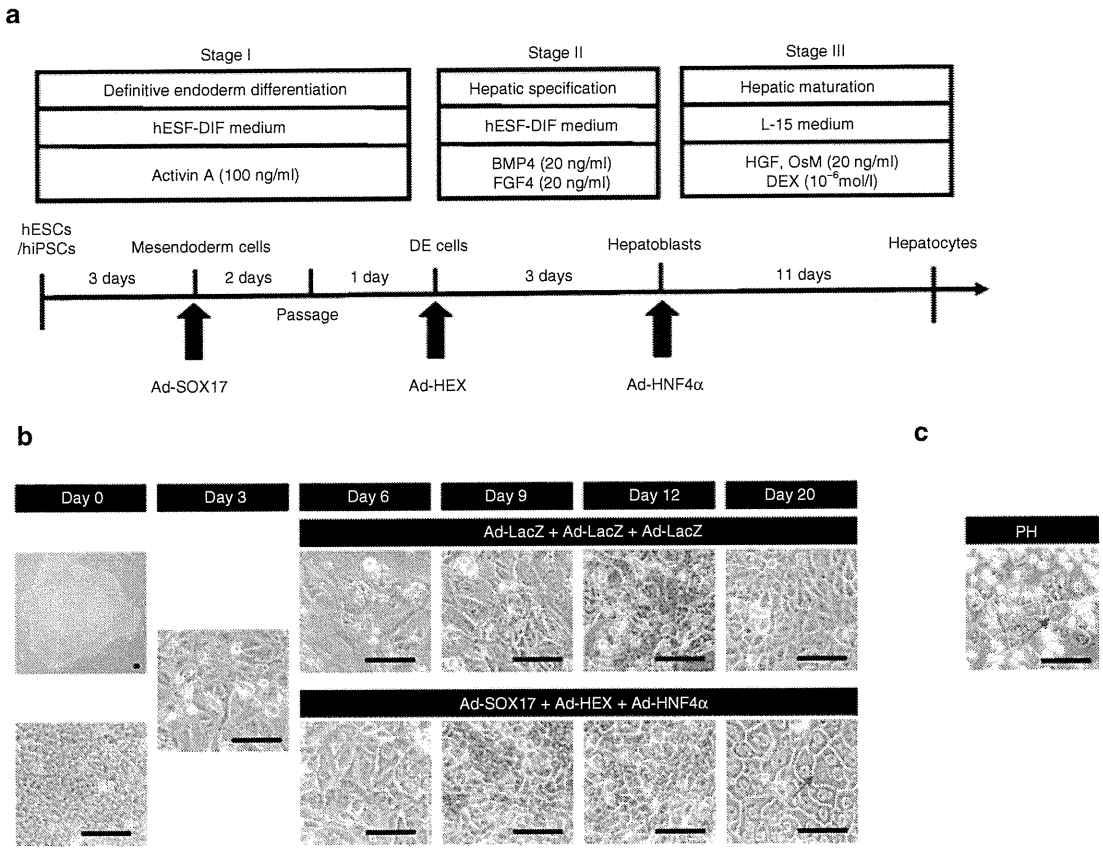

Figure 2 Hepatic differentiation of human ESCs and iPSCs transduced with three factors. (**a**) The procedure for differentiation of human ESCs and iPSCs into hepatocytes via DE cells and hepatoblasts is presented schematically. The hESF-DIF medium was supplemented with 10 μg/ml human recombinant insulin, 5 μg/ml human apotransferrin, 10 μmol/l 2-mercaptoethanol, 10 μmol/l ethanolamine, 10 μmol/l sodium selenite, and 0.5 mg/ml fatty-acid-free BSA. The L15 medium was supplemented with 8.3% tryptose phosphate broth, 8.3% FBS, 10 μmol/l hydrocortisone 21-hemisuccinate, 1 μmol/l insulin, and 25 mmol/l $NaHCO_3$. (**b**) Sequential morphological changes (day 0–20) of human ESCs (H9) differentiated into hepatocytes via DE cells and hepatoblasts are shown. Red arrow shows the cells that have double nuclei. (**c**) The morphology of primary human hepatocytes is shown. Bar represents 50 μm. BSA, bovine serum albumin; DE, definitive endoderm; ESC, embryonic stem cell; iPSC, induced pluripotent stem cell.

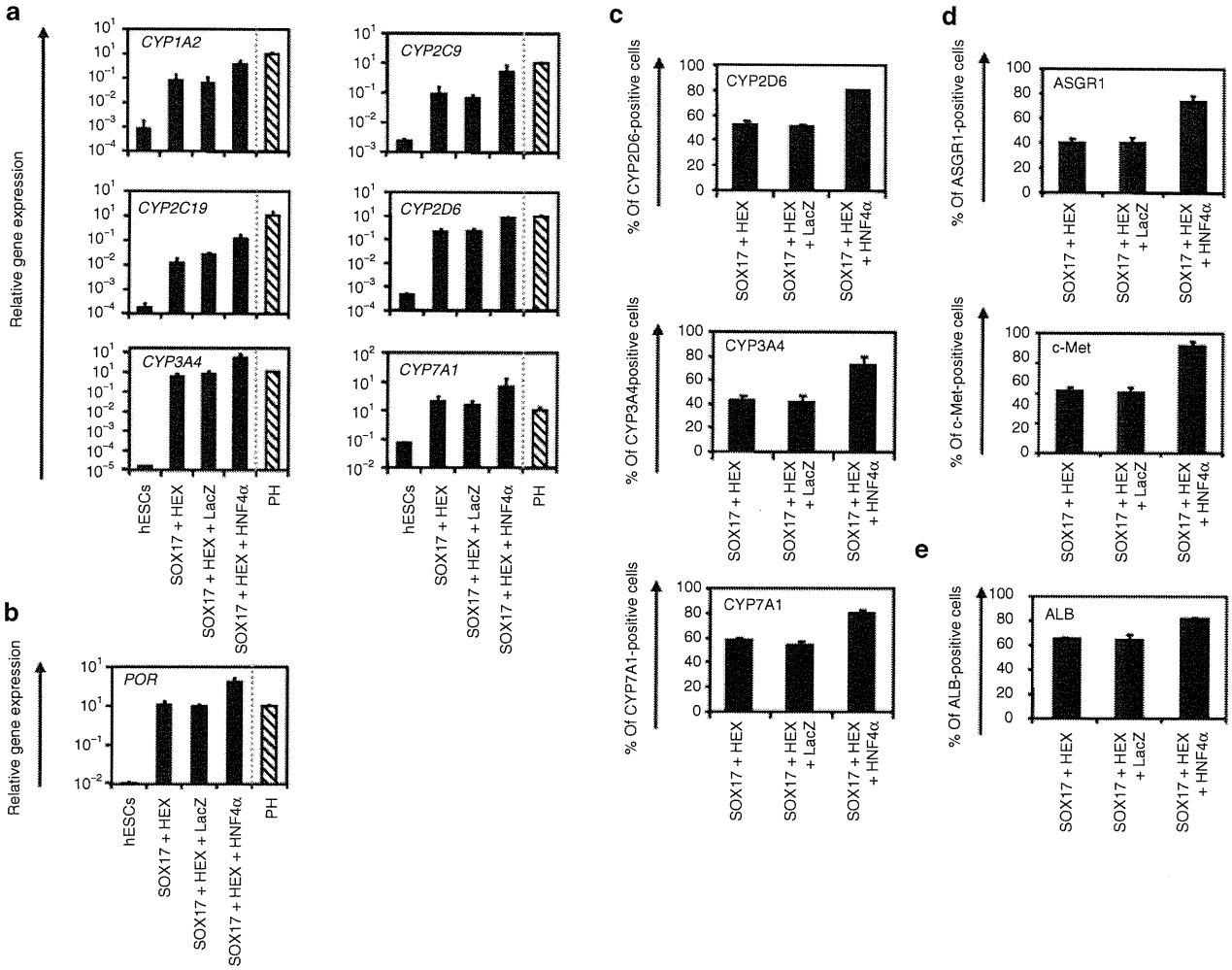

Figure 3 Transduction of HNF4α promotes hepatic maturation from human ESCs and iPSCs. (**a**,**b**) The human ESCs were differentiated into hepatocytes according to the protocol described in **Figure 2a**. On day 20 of differentiation, the gene expression levels of (**a**) CYP enzymes (*CYP1A2*, *CYP2C9*, *CYP2C19*, *CYP2D6*, *CYP3A4*, and *CYP7A1*) and (**b**) *POR* were examined by real-time RT-PCR in undifferentiated human ESCs (hESCs), the hepatocyte-like cells, and primary human hepatocytes (PH, hatched bar). On the y-axis, the expression level of primary human hepatocytes, which were cultured for 48 hours after the cells were plated, was taken as 1.0. (**c**–**e**) The hepatocyte-like cells (day 20) were subjected to immunostaining with (**c**) anti-drug-metabolizing enzymes (CYP2D6, CYP3A4, and CYP7A1), (**d**) anti-hepatic surface protein (ASGR1 and c-Met), and (**e**) anti-ALB antibodies, and then the percentage of antigen-positive cells was examined by flow cytometry on day 20 of differentiation. All data are represented as means ± SD (n = 3). ESC, embryonic stem cell; HNF4α, hepatocyte nuclear factor 4α; iPSC, induced pluripotent stem cell.

(POR)[26], which is required for the normal function of CYPs, was also higher in the three factors-transduced cells (**Figure 3b**). The gene expression analysis of ALB, α-1-antitrypsin (α-1-AT), transthyretin, hepatic conjugating enzymes, hepatic transporters, and hepatic transcription factors also showed higher expression levels in the three factors-transduced cells (**Supplementary Figures S7** and **S8**). Moreover, the gene expression levels of these hepatic markers of three factor-transduced cells were similar to those of primary human hepatocytes, although the levels depended on the type of gene (**Figure 3a,b**, and **Supplementary Figures S7** and **S8**). To confirm that similar results could be obtained with human iPSCs, we used three human iPS cell lines (201B7, Dotcom, and Tic). The gene expression of hepatic markers in human ESC- and iPSC-derived hepatocytes were analyzed by real-time reverse transcription-PCR on day 20 of differentiation. Three human iPS cell lines as well as human ESCs also effectively differentiated into hepatocytes in response to transduction of the three factors (**Supplementary Figure S9**). Interestingly, we observed differences in the hepatic maturation efficiency among the three human iPS cell lines. That is, two of the human iPS cell lines (Tic and Dotcom) were more committed to the hepatic lineage than another human iPS cell line (201B7). Because almost homogeneous hepatocyte-like cells would be more useful in basic research, regenerative medicine, and drug discovery, we also examined whether our novel methods for hepatic maturation could generate a homogeneous hepatocyte population by flow cytometry analysis (**Figure 3c–e**). The percentages of CYP2D6-, CYP3A4-, and CYP7A1-positive cells were ~80% in the three factors-transduced cells, while they were ~50% in the two factors-transduced cells (**Figure 3c**). The percentages of hepatic surface antigen (asialoglycoprotein receptor 1 (ASGR1] and met proto-oncogene (c-Met))-positive cells (**Figure 3d**) and ALB-positive cells (**Figure 3e**) were also ~80% in the three factors-transduced cells. These results indicated that a nearly homogeneous population was obtained by our differentiation protocol

using the transduction of three functional genes (SOX17, HEX, and HNF4α).

The three factors-transduced cells have characteristics of functional hepatocytes

The hepatic functions of the hepatocyte-like cells, such as the uptake of low-density lipoprotein (LDL) and CYP enzymes activity, of the hepatocyte-like cells were examined on day 20 of differentiation. Approximately 87% of the three factors-transduced cells uptook LDL in the medium, whereas only 44% of the two factors-transduced cells did so (**Figure 4a**). The activities of CYP enzymes of the hepatocyte-like cells were measured according to the metabolism of the CYP3A4, CYP2C9, or CYP1A2 substrates (**Figure 4b**). The metabolites were detected in the three factors-transduced cells and their activities were higher than those of the two factors-transduced cells (dimethyl sulfoxide (DMSO) column). We further tested the induction of CYP3A4, CYP2C9, and CYP1A2 by chemical stimulation, since CYP3A4, CYP2C9, and CYP1A2 are the important prevalent CYP isozymes in the liver and are involved in the metabolism of a significant proportion of the currently available commercial drugs (rifampicin or omeprazole column). It is well known that CYP3A4 and CYP2C9 can be induced by rifampicin, whereas CYP1A2 can be induced by omeprazole. The hepatocyte-like cells were treated with either of these. Although undifferentiated human ESCs responsed to neither rifampicin nor omeprazole (data not shown), the hepatocyte-like cells produced more metabolites in response to chemical stimulation as well as primary hepatocytes (**Figure 4b**). The activity levels of the hepatocyte-like cells as compared with those of primary human hepatocytes depended on the types of CYP; the CYP3A4 activity of the hepatocyte-like cells was similar to that of primary human hepatocytes, whereas the CYP2C9 and CYP1A2 activities of the hepatocyte-like cells were slightly lower than those of primary human hepatocytes (**Figure 3a**). These results indicated that high levels of functional CYP enzymes were detectable in the hepatocyte-like cells.

The metabolism of diverse compounds involving uptake, conjugation, and the subsequent release of the compounds is an important function of hepatocytes. Uptake and release of Indocyanine green (ICG) can often be used to identify hepatocytes in ESC differentiation models.[27] To investigate this function in our hepatocyte-like cells, we compared this ability of the three factors-transduced cells with that of the two factors-transduced cells on day 20 of differentiation (**Figure 4c**). The three factors-transduced cells had more ability to uptake ICG and to excrete ICG by culturing without ICG for 6 hours. We also examined whether the hepatocyte-like cells could store glycogen, a characteristic of functional hepatocytes (**Figure 4d**). On day 20 of differentiation, the three factors-transduced cells and the two factors-transduced cells were stained for cytoplasmic glycogen using the Periodic Acid-Schiff staining procedure. The three factors-transduced cells exhibited more abundant storage of glycogen than the two-factors-transduced cells. These results showed that abundant hepatic functions, such as uptake and excretion of ICG and storage of glycogen, were obtained by the transduction of three factors.

Many adverse drug reactions are caused by the CYP-dependent activation of drugs into reactive metabolites.[28] In order to examine metabolism-mediated toxicity and to improve the safety of drug candidates, primary human hepatocytes are widely used.[28] Because primary human hepatocytes have quite different characteristics among distinct lots and because it is difficult to purchase large amounts of primary human hepatocytes that have the same characteristics, hepatocyte-like cells are expected to be used for this purpose. To examine whether our hepatocyte-like cells could be used to predict metabolism-mediated toxicity, the hepatocyte-like cells were incubated with four substrates (troglitazone, acetaminophen, cyclophosphamide, and carbamazepine), which are known to generate toxic metabolites by CYP enzymes, and then the cell viability was measured (**Figure 4e**). The cell viability of the two factors plus Ad-LacZ-tansduced cells were higher than that of the three factors-transduced cells at each different concentration of four test compounds. These results indicated that the three factors-transduced cells could more efficiently metabolize the test compounds and thereby induce higher toxicity than either the two factors-transduced cells or undifferentiated human ESCs. The cell viability of the three factors-transduced cells was slightly higher than that of primary human hepatocytes.

HNF4α promotes hepatic maturation by activating mesenchymal-to-epithelial transition

HNF4α is known as a dominant regulator of the epithelial phenotype because its ectopic expression in fibroblasts (such as NIH 3T3 cells) induces mesenchymal-to-epithelial transition (MET)[11], although it is not known whether HNF4α can promote MET in hepatic differentiation. Therefore, we examined whether HNF4α transduction promotes hepatic maturation from hepatoblasts by activating MET. To clarify whether MET is activated by HNF4α transduction, the human ESC-derived hepatoblasts (day 9) were transduced with Ad-LacZ or Ad-HNF4α, and the resulting phenotype was analyzed on day 12 of differentiation (**Figure 5**). This time, we confirmed that HNF4α transduction decreased the population of N-cadherin (hepatoblast marker)-positive cells,[29] whereas it increased that of ALB (hepatocyte marker)-positive cells (**Figure 5a**). The number of CK7 (cholangiocyte marker)-positive population did not change (**Figure 5a**). To investigate whether these results were attributable to MET, the alteration of the expression of several mesenchymal and epithelial markers was examined (**Figure 5b**). The human ESC-derived hepatoblasts (day 9) were almost homogeneously N-cadherin[30] (mesenchymal marker)-positive and E-cadherin[11] (epithelial marker)-negative, demonstrating that human ESC-derived hepatoblasts have mesenchymal characteristics (**Figure 5a,b**). After HNF4α transduction, the number of E-cadherin-positive cells was increased and reached ~90% on day 20, whereas that of N-cadherin-positive cells was decreased and was less than 5% on day 20 (**Supplementary Figure S10**). These results indicated that MET was promoted by HNF4α transduction in hepatic differentiation from hepatoblasts. Interestingly, the number of growing cells was decreased by HNF4α transduction (**Figure 5c**), and the cell growth was delayed by HNF4α transduction (**Supplementary Figure S11**). This decrease in the number of growing cells might have been because the differentiation was promoted by HNF4α transduction. We also confirmed that MET was promoted by HNF4α transduction in the gene expression levels (**Figure 5d**).

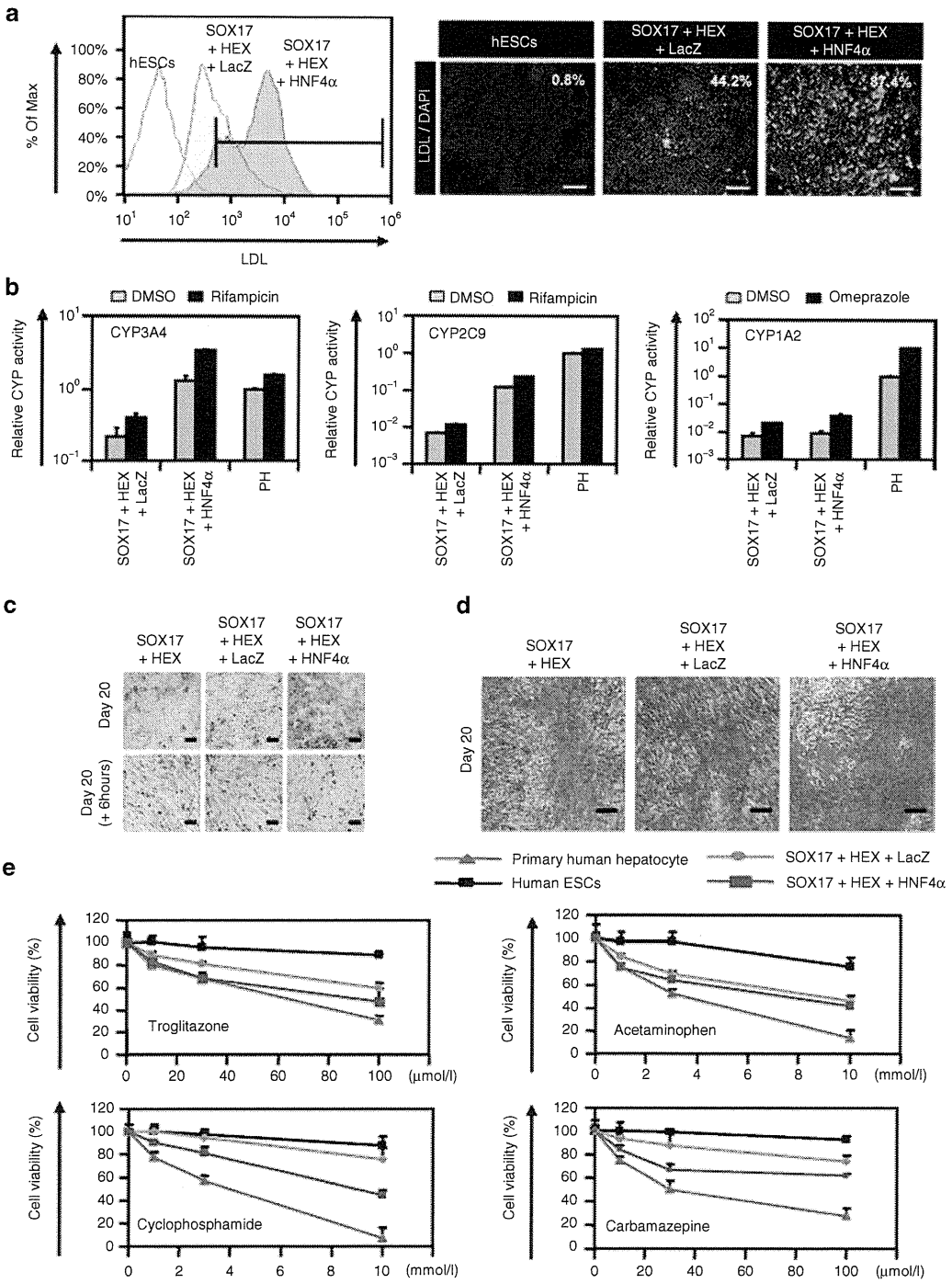

Figure 4 Transduction of the three factors enhances hepatic functions. The human ESCs were differentiated into hepatoblasts and transduced with 3,000 VP/cell of Ad-LacZ or Ad-HNF4α for 1.5 hours and cultured until day 20 of differentiation according to the protocol described in **Figure 2a**. The hepatic functions of the two factors plus Ad-LacZ-transduced cells (SOX17+HEX+LacZ) and the three factors-transduced cells (SOX17+HEX+HNF4α) were compared. (**a**) Undifferentiated human ESCs (hESCs) and the hepatocyte-like cells (day 20) were cultured with medium containing Alexa-Flour 488-labeled LDL (green) for 1 hour, and immunohistochemistry and flow cytometry analysis were performed. The percentage of LDL-positive cells was measured by flow cytometry. Nuclei were counterstained with DAPI (blue). The bar represents 100 μm. (**b**) Induction of CYP3A4 (left), CYP2C9 (middle), or CYP1A2 (right) by DMSO (gray bar), rifampicin (black bar), or omeprazole (black bar) in the hepatocyte-like cells (day 20) and primary human hepatocytes (PH), which were cultured for 48 hours after the cells were plated. On the y-axis, the activity of primary human hepatocytes that have been cultured with medium containing DMSO was taken as 1.0. (**c**) The hepatocyte-like cells (day 20) (upper column) were examined for their ability to take up Indocyanin Green (ICG) and release it 6 hours thereafter (lower column). (**d**) Glycogen storage of the hepatocyte-like cells (day 20) was assessed by Periodic Acid-Schiff (PAS) staining. PAS staining was performed on day 20 of differentiation. Glycogen storage is indicated by pink or dark red-purple cytoplasms. The bar represents 100 μm. (**e**) The cell viability of undifferentiated human ESCs (black), two factors plus Ad-LacZ-tansduced cells (green), the three factors-transduced cells (blue), and primary human hepatocytes (red) was assessed by Alamar Blue assay after 48 hours exposure to different concentrations of four test compounds (troglitazone, acetaminophen, cyclophosphamide, and carbamazepine). The cell viability is expressed as a percentage of cells treated with solvent only treat: 0.1% DMSO except for carbamazepine: 0.5% DMSO. All data are represented as means ± SD (n = 3). ESC, embryonic stem cell; DMSO, dimethyl sulfoxide; LDL, low-density lipoprotein.

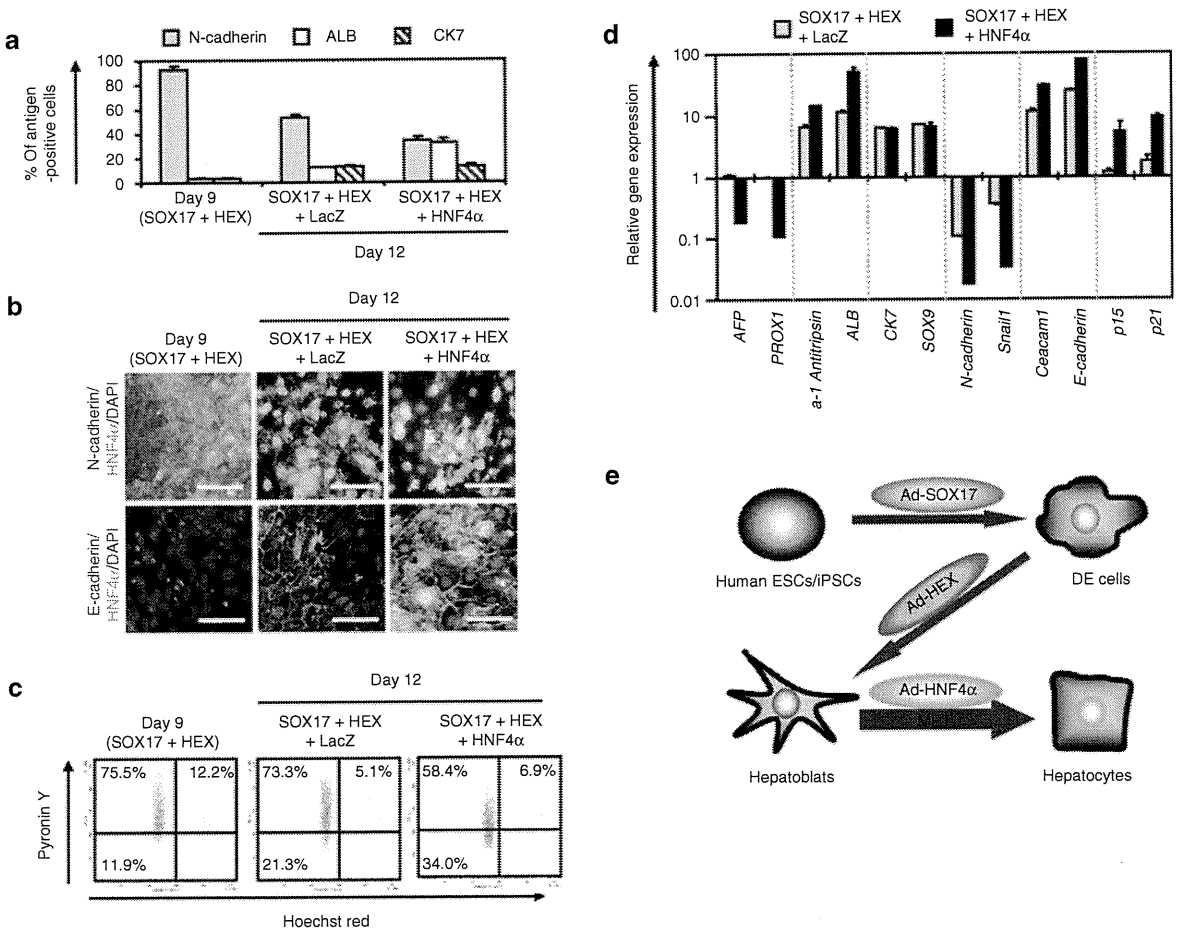

Figure 5 HNF4α promotes hepatic differentiation by activating MET. Human ESCs were differentiated into hepatoblasts according to the protocol described in **Figure 2a**, and then transduced with 3,000 VP/cell of Ad-LacZ or Ad-HNF4α for 1.5 hours, and finally cultured until day 12 of differentiation. (**a**) The hepatoblasts, two factors plus Ad-LacZ-transduced cells (SOX17+HEX+LacZ) (day 12), and the three factors-transduced cells (SOX17+HEX+HNF4α) (day 12) were subjected to immunostaining with anti-N-cadherin, ALB, or CK7 antibodies. The percentage of antigen-positive cells was measured by flow cytometry. (**b**) The cells were subjected to immunostaining with anti-N-cadherin (green), E-cadherin (green), or HNF4α (red) antibodies on day 9 or day 12 of differentiation. Nuclei were counterstained with DAPI (blue). The bar represents 50 μm. Similar results were obtained in two independent experiments. (**c**) The cell cycle was examined on day 9 or day 12 of differentiation. The cells were stained with Pyronin Y (y-axis) and Hoechst 33342 (x-axis) and then analyzed by flow cytometry. The growth fraction of cells is the population of actively dividing cells (G1/S/G2/M). (**d**) The expression levels of *AFP*, *PROX1*, *α-1-antitrypsin*, *ALB*, *CK7*, *SOX9*, *N-cadherin*, *Snail1*, *Ceacam1*, *E-cadherin*, *p15*, and *p21* were examined by real-time RT-PCR on day 9 or day 12 of differentiation. The expression level of hepatoblasts (day 9) was taken as 1.0. All data are represented as means ± SD ($n = 3$). (**e**) The model of efficient hepatic differentiation from human ESCs and iPSCs in this study is summarized. The human ESCs and iPSCs differentiate into hepatocytes via definitive endoderm and hepatoblasts. At each stage, the differentiation is promoted by stage-specific transduction of appropriate functional genes. In the last stage of hepatic differentiation, HNF4α transduction provokes hepatic maturation by activating MET. ESC, embryonic stem cell; HNF4α, hepatocyte nuclear factor 4α; iPSC, induced pluripotent stem cell; MET, mesenchymal-to-epithelial transition; RT-PCR, reverse transcription-PCR; VP, vector particle.

The gene expression levels of hepatocyte markers (*α-1-antitrypsin* and *ALB*)[20] and epithelial markers (*Ceacam1* and *E-cadherin*) were upregulated by HNF4α transduction. On the other hand, the gene expression levels of hepatoblast markers (*AFP* and *PROX1*)[31], mesenchymal markers (*N-cadherin* and *Snail*)[32], and cyclin dependent kinase inhibitor (*p15* and *p21*)[33] were downregulated by HNF4α transduction. HNF4α transduction did not change the expression levels of cholangiocyte markers (*CK7* and *SOX9*). We conclude that HNF4α promotes hepatic maturation by activating MET.

DISCUSSION

This study has two main purposes: the generation of functional hepatocytes from human ESCs and iPSCs for application to drug toxicity screening in the early phase of pharmaceutical development and; elucidation of the HNF4α function in hepatic maturation from human ESCs. We initially confirmed the importance of transcription factor HNF4α in hepatic differentiation from human ESCs by using a published data set of gene array analysis (**Supplementary Figure S1**).[34] We speculated that HNF4α transduction could enhance hepatic differentiation from human ESCs and iPSCs.

To generate functional hepatocytes from human ESCs and iPSCs and to elucidate the function of HNF4α in hepatic differentiation from human ESCs, we examined the stage-specific roles of HNF4α. We found that hepatoblast (day 9) stage-specific HNF4α transduction promoted hepatic differentiation (**Figure 1**). Because endogenous HNF4α is initially expressed in the hepatoblast,[9,10] our system might adequately reflect early embryogenesis. However, HNF4α transduction at an inappropriate stage (day 6 or day 12) promoted

bidirectional differentiation; heterogeneous populations, which contain the hepatocytes and pancreas cells or hepatocytes and cholangiocytes, were obtained, respectively (**Figure 1**), consistent with a previous report that HNF4α plays an important role not only in the liver but also in the pancreas.[12] Therefore, we concluded that HNF4α plays a significant stage-specific role in the differentiation of human ESC- and iPSC-derived hepatoblasts to hepatocytes (**Figure 5e**).

We found that the expression levels of the hepatic functional genes were upregulated by HNF4α transduction (**Figure 3a,b**, and **Supplementary Figures S7** and **S8**). Although the c/EBPα and GATA4 expression levels of the three factors-transduced cells were higher than those of primary human hepatocytes, the FOXA1, FOXA2, FOXA3, and HNF1α, which are known to be important for hepatic direct reprogramming and hepatic differentiation,[35,36] expression levels of three factors-transduced cells were slightly lower than those of primary human hepatocytes (**Supplementary Figure S8**). Therefore, additional transduction of FOXA1, FOXA2, FOXA3, and HNF1α might promote further hepatic maturation. Some previous hepatic differentiation protocols that utilized growth factors without gene transfer led to the appearance only of heterogeneous hepatocyte populations.[4–6] The HNF4α transduction led not only to the upregulation of expression levels of several hepatic markers but also to an almost homogeneous hepatocyte population; the differentiation efficacy based on CYPs, ASGR1, or ALB expression was ~80% (**Figure 3c–e**). The efficient hepatic maturation in this study might be attributable to the activation of many hepatocyte-associated genes by the transduction of HNF4α, which binds to the promoters of nearly half of the genes expressed in the liver.[12] In the later stage of hepatic maturation, hepatocyte-associated genes would be strongly upregulated by endogenous transcription factors but not exogenous HNF4α because transgene expression by Ad vectors was almost disappeared on day 18 (**Supplementary Figure S5**). Another reason for the efficient hepatic maturation would be that sequential transduction of SOX17, HEX, and HNF4α could mimic hepatic differentiation in early embryogenesis.

Next, we examined whether or not the hepatocyte-like cells had hepatic functions. The activity of many kinds of CYPs was upregulated by HNF4α transduction (**Figure 4b**). Ad-HNF4α-transduced cells exhibit many characteristics of hepatocytes: uptake of LDL, uptake and excretion of ICG, and storage of glycogen (**Figure 4a,c,d**). Many conventional tests of hepatic characteristics have shown that the hepatocyte-like cells have mature hepatocyte functions. Furthermore, the hepatocyte-like cells can catalyze the toxication of several compounds (**Figure 4e**). Although the activities to catalyze the toxication of test compounds in primary human hepatocytes are slightly higher than those in the hepatocyte-like cells, the handling of primary human hepatocytes is difficult for a number of reasons: since their source is limited, large-scale primary human hepatocytes are difficult to prepare as a homogeneous population. Therefore, the hepatocyte-like cells derived from human ESCs and iPSCs would be a valuable tool for predicting drug toxicity. To utilize the hepatocyte-like cells in a drug toxicity study, further investigation of the drug metabolism capacity and CYP induction potency will be needed.

We also investigated the mechanisms underlying efficient hepatic maturation by HNF4α transduction. Although the number of cholangiocyte populations did not change by HNF4α transduction, we found that the number of hepatoblast populations decreased and that of hepatocyte populations increased, indicating that HNF4α promotes selective hepatic differentiation from hepatoblasts (**Figure 5a**). As previously reported, HNF4α regulates the expression of a broad range of genes that code for cell adhesion molecules,[13] extracellular matrix components, and cytoskeletal proteins, which determine the main morphological characteristics of epithelial cells.[14,35,37] In this study, we elucidated that MET was promoted by HNF4α transduction (**Figure 5b,d**). Thus, we conclude that HNF4α overexpression in hepatoblasts promotes hepatic differentiation by activating MET (**Figure 5e**).

Using human iPSCs as well as human ESCs, we confirmed that the stage-specific overexpression of HNF4α could promote hepatic maturation (**Supplementary Figure S9**). Interestingly, the differentiation efficacies differed among human iPS cell lines: two of the human iPS cell lines (Dotcom and Tic) were more committed to the hepatic lineage than another human iPS cell line (201B7) (**Supplementary Figure S7**). Therefore, it would be necessary to select a human iPS cell line that is suitable for hepatic maturation in the case of medical applications, such as drug screening and liver transplantation. The difference of hepatic differentiation efficacy among the three iPSC lines might be due to the difference of epigenetic memory of original cells or the difference of the inserted position of the foreign genes for the reprogramming.

To control hepatic differentiation mimicking embryogenesis, we employed Ad vectors, which are one of the most efficient transient gene delivery vehicles and have been widely used in both experimental studies and clinical trials.[38] We used a fiber-modified Ad vector containing the EF-1α promoter and a stretch of lysine residue (KKKKKKK, K7) peptides in the C-terminal region of the fiber knob.[19] The K7 peptide targets heparan sulfates on the cellular surface, and the fiber-modified Ad vector containing the K7 peptides was shown to be efficient for transduction into many kinds of cells including human ESCs and human ESC-derived cells.[7–8,19] Thus, Ad vector-mediated transient gene transfer should be a powerful tool for regulating cellular differentiation.

In summary, the findings described here demonstrate that transcription factor HNF4α plays a crucial role in the hepatic differentiation from human ESC-derived hepatoblasts by activating MET (**Figure 5e**). In the present study, both human ESCs and iPSCs (three lines) were used and all cell lines showed efficient hepatic maturation, indicating that our protocol would be a universal tool for cell line-independent differentiation into functional hepatocytes. Moreover, the hepatocyte-like cells can catalyze the toxication of several compounds as primary human hepatocytes. Therefore, our technology, by sequential transduction of SOX17, HEX, and HNF4α, would be a valuable tool for the efficient generation of functional hepatocytes derived from human ESCs and iPSCs, and the hepatocyte-like cells could be used for the prediction of drug toxicity.

MATERIALS AND METHODS

Human ESC and iPSC culture. A human ES cell line, H9 (WiCell Research Institute, Madison, HI), was maintained on a feeder layer of mitomycin C-treated mouse embryonic fibroblasts (Millipore, Billerica, MA) with Repro Stem (Repro CELL, Tokyo, Japan) supplemented with 5 ng/ml fibroblast

growth factor 2 (FGF2) (Sigma, St Louis, MO). Human ESCs were dissociated with 0.1 mg/ml dispase (Roche Diagnostics, Indianapolis, IN) into small clumps and then were subcultured every 4 or 5 days. H9 was used following the Guidelines for Derivation and Utilization of Human Embryonic Stem Cells of the Ministry of Education, Culture, Sports, Science and Technology of Japan. Two human iPS cell lines generated from the human embryonic lung fibroblast cell line MCR5 were provided from the JCRB Cell Bank (Tic, JCRB Number: JCRB1331; and Dotcom, JCRB Number: JCRB1327).[39,40] These human iPS cell lines were maintained on a feeder layer of mitomycin C-treated mouse embryonic fibroblasts with iPSellon (Cardio, Kobe, Japan) supplemented with 10 ng/ml FGF2. Another human iPS cell line, 201B7, generated from human dermal fibroblasts was kindly provided by Dr S. Yamanaka (Kyoto University).[2] The human iPS cell line 201B7 was maintained on a feeder layer of mitomycin C-treated mouse embryonic fibroblasts with Repro Stem (Repro CELL) supplemented with 5 ng/ml FGF2 (Sigma). Human iPSCs were dissociated with 0.1 mg/ml dispase (Roche Diagnostics) into small clumps and were then subcultured every 5 or 6 days.

In vitro *differentiation.* Before the initiation of cellular differentiation, the medium of human ESCs and iPSCs was exchanged for a defined serum-free medium, hESF9, and cultured as we previously reported.[41] hESF9 consists of hESF-GRO medium (Cell Science & Technology Institute, Sendai, Japan) supplemented with 10 μg/ml human recombinant insulin, 5 μg/ml human apotransferrin, 10 μmol/l 2-mercaptoethanol, 10 μmol/l ethanolamine, 10 μmol/l sodium selenite, oleic acid conjugated with fatty-acid-free bovine albumin (BSA), 10 ng/ml FGF2, and 100 ng/ml heparin (all from Sigma).

The differentiation protocol for the induction of DE cells, hepatoblasts, and hepatocytes was based on our previous report with some modifications.[7] Briefly, in mesendoderm differentiation, human ESCs and iPSCs were dissociated into single cells and cultured for 3 days on Matrigel (Becton, Dickinson and Company, Tokyo, Japan) in hESF-DIF medium (Cell Science & Technology Institute) supplemented with 10 μg/ml human recombinant insulin, 5 μg/ml human apotransferrin, 10 μmol/l 2-mercaptoethanol, 10 μmol/l ethanolamine, 10 μmol/l sodium selenite, 0.5 mg/ml BSA, and 100 ng/ml Activin A (R&D Systems, Minneapolis, MN). To generate mesendoderm cells and DE cells, human ESC-derived cells were transduced with 3,000 vector particles (VP)/cell of Ad-SOX17 for 1.5 hours on day 3 and cultured until day 6 on Matrigel (BD) in hESF-DIF medium (Cell Science & Technology Institute) supplemented with 10 μg/ml human recombinant insulin, 5 μg/ml human apotransferrin, 10 μmol/l 2-mercaptoethanol, 10 μmol/l ethanolamine, 10 μmol/l sodium selenite, 0.5 mg/ml BSA, and 100 ng/ml Activin A (R&D Systems). For induction of hepatoblasts, the DE cells were transduced with 3,000 VP/cell of Ad-HEX for 1.5 hours on day 6 and cultured for 3 days on a Matrigel (BD) in hESF-DIF (Cell Science & Technology Institute) medium supplemented with the 10 μg/ml human recombinant insulin, 5 μg/ml human apotransferrin, 10 μmol/l 2-mercaptoethanol, 10 μmol/l ethanolamine, 10 μmol/l sodium selenite, 0.5 mg/ml BSA, 20 ng/ml bone morphogenetic protein 4 (R&D Systems), and 20 ng/ml FGF4 (R&D Systems). In hepatic differentiation, hepatoblasts were transduced with 3,000 VP/cell of Ad-LacZ or Ad-HNF4α for 1.5 hr on day 9 and were cultured for 11 days on Matrigel (BD) in L15 medium (Invitrogen, Carlsbad, CA) supplemented with 8.3% tryptose phosphate broth (BD), 8.3% fetal bovine serum (Vita, Chiba, Japan), 10 μmol/l hydrocortisone 21-hemisuccinate (Sigma), 1 μmol/l insulin, 25 mmol/l $NaHCO_3$ (Wako, Osaka, Japan), 20 ng/ml hepatocyte growth factor (R&D Systems), 20 ng/ml Oncostatin M (R&D Systems), and 10^{-6} mol/l Dexamethasone (Sigma).

Ad vectors. Ad vectors were constructed by an improved *in vitro* ligation method.[42,43] The human HNF4α gene (accession number NM_000457) was amplified by PCR using primers designed to incorporate the 5′ Not I and 3′ Xba I restriction enzyme sites: Fwd 5′-ggcctctagatggaggcagggagaatg-3′ and Rev 5′-ccccgcggccgcagcggcttgctagataac-3′. The human HNF4α gene was inserted into pBSKII (Invitrogen), resulting in pBSKII-HNF4α, and then the human HNF4α gene was inserted into pHMEF5,[44] which contains the human elongation factor-1α (EF-1α) promoter, resulting in pHMEF-HNF4α. The pHMEF-HNF4α was digested with I-CeuI/PI-SceI and ligated into I-Ceu I/PI-SceI-digested pAdHM41-K7,[19] resulting in pAd-HNF4α. The human EF-1α promoter-driven LacZ-, SOX17-, or HEX-expressing Ad vectors, Ad-LacZ, Ad-SOX17, or Ad-HEX, were constructed previously.[7,8,45] Ad-LacZ, Ad-SOX17, Ad-HEX, and Ad-HNF4α, each of which contains a stretch of lysine residue (K7) peptides in the C-terminal region of the fiber knob for more efficient transduction of human ESCs, iPSCs, and DE cells, were generated and purified as described previously.[7] The VP titer was determined by using a spectrophotometric method.[46]

LacZ assay. Human ESC- and iPSC-derived cells were transduced with Ad-LacZ at 3,000 VP/cell for 1.5 hours. After culturing for the indicated number of days, 5-bromo-4-chloro-3-indolyl β-D-galactopyranoside (X-Gal) staining was performed as described previously.[44]

Flow cytometry. Single-cell suspensions of human ESCs, iPSCs, and their derivatives were fixed with methanol at 4 °C for 20 minutes and then incubated with the primary antibody, followed by the secondary antibody. Flow cytometry analysis was performed using a FACS LSR Fortessa flow cytometer (BD).

RNA isolation and reverse transcription-PCR. Total RNA was isolated from human ESCs, iPSCs, and their derivatives using ISOGENE (Nippon Gene) according to the manufacturer's instructions. Primary human hepatocytes were purchased from CellzDirect, Durham, NC. complementary DNA was synthesized using 500 ng of total RNA with a Superscript VILO cDNA synthesis kit (Invitrogen). Real-time reverse transcription-PCR was performed with Taqman gene expression assays (Applied Biosystems, Foster City, CA) or SYBR Premix Ex Taq (TaKaRa) using an ABI PRISM 7000 Sequence Detector (Applied Biosystems). Relative quantification was performed against a standard curve and the values were normalized against the input determined for the housekeeping gene, glyceraldehyde 3-phosphate dehydrogenase. The primer sequences used in this study are described in **Supplementary Table S1**.

Immunohistochemistry. The cells were fixed with methanol or 4% paraformaldehyde (Wako). After blocking with phosphate-buffered saline containing 2% BSA (Sigma) and 0.2% Triton X-100 (Sigma), the cells were incubated with primary antibody at 4 °C for 16 hours, followed by incubation with a secondary antibody that was labeled with Alexa Fluor 488 (Invitrogen) or Alexa Fluor 594 (Invitrogen) at room temperature for 1 hour. All the antibodies are listed in **Supplementary Table S2**.

Assay for CYP activity. To measure cytochrome P450 3A4, 2C9, and 1A2 activity, we performed Lytic assays by using a P450-GloTM CYP3A4 Assay Kit (Promega, Madison, WI). For the CYP3A4 and 2C9 activity assay, undifferentiated human ESCs, the hepatocyte-like cells, and primary human hepatocytes were treated with rifampicin (Sigma), which is the substrate for CYP3A4 and CYP2C9, at a final concentration of 25 μmol/l or DMSO (0.1%) for 48 hours. For the CYP1A2 activity assay, undifferentiated human ESCs, the hepatocyte-like cells, and primary human hepatocytes were treated with omeprazole (Sigma), which is the substrate for CYP1A2, at a final concentration of 10 μM or DMSO (0.1%) for 48 hours. We measured the fluorescence activity with a luminometer (Lumat LB 9507; Berthold, Oak Ridge, TN) according to the manufacturer's instructions.

Pyronin Y/Hoechst Staining. Human ESC-derived cells were stained with Hoechst33342 (Sigma) and Pyronin Y (PY) (Sigma) in Dulbecco's modified Eagle medium (Wako) supplemented with 0.2 mmol/l HEPES and 5% FCS (Invitrogen). Samples were then placed on ice for 15 minutes, and 7-AAD was added to a final concentration of 0.5 mg/ml for exclusion of dead cells. Fluorescence-activated cell-sorting analysis of these cells was

performed on a FACS LSR Fortessa flow cytometer (Becton Dickinson) equipped with a UV-laser.

Cellular uptake and excretion of ICG. ICG (Sigma) was dissolved in DMSO at 100 mg/ml, then added to a culture medium of the hepatocyte-like cells to a final concentration of 1 mg/ml on day 20 of differentiation. After incubation at 37 °C for 60 minutes, the medium with ICG was discarded and the cells were washed with phosphate-buffered saline. The cellular uptake of ICG was then examined by microscopy. Phosphate-buffered saline was then replaced by the culture medium and the cells were incubated at 37 °C for 6 hours. The excretion of ICG was examined by microscopy.

Periodic Acid-Schiff assay for glycogen. The hepatocyte-like cells were fixed with 4% paraformaldehyde and stained using a Periodic Acid-Schiff staining system (Sigma) on day 20 of differentiation according to the manufacturer's instructions.

Cell viability tests. Cell viability was assessed by Alamar Blue assay kit (Invitrogen). After treatment with test compounds[47–50] (troglitazone, acetaminophen, cyclophosphamide, and carbamazepine) (all from Wako) for 2 days, the culture medium was replaced with 0.5 mg/ml solution of Alamar Blue in culturing medium and cells were incubated for 3 hours at 37 °C. The supernatants of the cells were measured at a wavelength of 570 nm with background subtraction at 600 nm in a plate reader. Control refers to incubations in the absence of test compounds and was considered as 100% viability value.

Uptake of LDL. The hepatocyte-like cells were cultured with medium containing Alexa-488-labeled LDL (Invitrogen) for 1 hour, and then the cells that could uptake LDL were assessed by immunohistochemistry and flow cytometry.

Primary human hepatocytes. Cryopreserved human hepatocytes were purchased from CellzDirect (lot Hu8072). The vials of hepatocytes were rapidly thawed in a shaking water bath at 37 °C; the contents of the vial were emptied into prewarmed Cryopreserved Hepatocyte Recovery Medium (CellzDirect) and the suspension was centrifuged at 100*g* for 10 minutes at room temperature. The hepatocytes were seeded at 1.25×10^5 cells/cm^2 in hepatocyte culture medium (Lonza, Walkersville, MD) containing 10% FCS (GIBCO-BRL) onto type I collagen-coated 12-well plates. The medium was replaced with hepatocyte culture medium containing 10% FCS (GIBCO-BRL) 6 hours after seeding. The hepatocytes, which were cultured 48 hours after plating the cells, were used in the experiments.

SUPPLEMENTARY MATERIAL

Figure S1. Genome-wide screening of transcription factors involved in hepatic differentiation emphasizes the importance of the transcription factor HNF4α.
Figure S2. Summary of specific markers for DE cells, hepatoblasts, hepatocytes, cholangiocytes, and pancreas cells.
Figure S3. The formation of DE cells, hepatoblasts, hepatocytes, and cholangiocytes from human ESCs.
Figure S4. Overexpression of HNF4α mRNA in hepatoblasts by Ad-HNF4α transduction.
Figure S5. Time course of LacZ expression in hepatoblasts transduced with Ad-LacZ.
Figure S6. The morphology of the hepatocyte-like cells.
Figure S7. Upregulation of the expression levels of conjugating enzymes and hepatic transporters by HNF4α transduction.
Figure S8. Upregulation of the expression levels of hepatic transcription factors by HNF4α transduction.
Figure S9. Generation of hepatocytes from various human ES or iPS cell lines.
Figure S10. Promotion of MET by HNF4α transduction.
Figure S11. Arrest of cell growth by HNF4α transduction.
Table S1. List of Taqman probes and primers used in this study.
Table S2. List of antibodies used in this study.

ACKNOWLEDGMENTS

We thank Hiroko Matsumura and Misae Nishijima for their excellent technical support. H.M., M.K.F., and T.H. were supported by grants from the Ministry of Health, Labor, and Welfare of Japan. H.M. was also supported by Japan Research foundation For Clinical Phamacology, The Nakatomi Foundation, and The Uehara Memorial Foundation. K.K. (K. Kawabata) was supported by grants from the Ministry of Education, Sports, Science and Technology of Japan (20200076) and the Ministry of Health, Labor, and Welfare of Japan. K.K. (K. Katayama) and F.S. was supported by Program for Promotion of Fundamental Studies in Health Sciences of the National Institute of Biomedical Innovation (NIBIO).

REFERENCES

1. Thomson, JA, Itskovitz-Eldor, J, Shapiro, SS, Waknitz, MA, Swiergiel, JJ, Marshall, VS *et al.* (1998). Embryonic stem cell lines derived from human blastocysts. *Science* **282**: 1145–1147.
2. Takahashi, K, Tanabe, K, Ohnuki, M, Narita, M, Ichisaka, T, Tomoda, K *et al.* (2007). Induction of pluripotent stem cells from adult human fibroblasts by defined factors. *Cell* **131**: 861–872.
3. Murry, CE and Keller, G (2008). Differentiation of embryonic stem cells to clinically relevant populations: lessons from embryonic development. *Cell* **132**: 661–680.
4. Basma, H, Soto-Gutiérrez, A, Yannam, GR, Liu, L, Ito, R, Yamamoto, T *et al.* (2009). Differentiation and transplantation of human embryonic stem cell-derived hepatocytes. *Gastroenterology* **136**: 990–999.
5. Touboul, T, Hannan, NR, Corbineau, S, Martinez, A, Martinet, C, Branchereau, S *et al.* (2010). Generation of functional hepatocytes from human embryonic stem cells under chemically defined conditions that recapitulate liver development. *Hepatology* **51**: 1754–1765.
6. Duan, Y, Ma, X, Ma, X, Zou, W, Wang, C, Bahbahan, IS *et al.* (2010). Differentiation and characterization of metabolically functioning hepatocytes from human embryonic stem cells. *Stem Cells* **28**: 674–686.
7. Inamura, M, Kawabata, K, Takayama, K, Tashiro, K, Sakurai, F, Katayama, K *et al.* (2011). Efficient generation of hepatoblasts from human ES cells and iPS cells by transient overexpression of homeobox gene HEX. *Mol Ther* **19**: 400–407.
8. Takayama, K, Inamura, M, Kawabata, K, Tashiro, K, Katayama, K, Sakurai, F *et al.* (2011). Efficient and directive generation of two distinct endoderm lineages from human ESCs and iPSCs by differentiation stage-specific SOX17 transduction. *PLoS ONE* **6**: e21780.
9. Duncan, SA, Manova, K, Chen, WS, Hoodless, P, Weinstein, DC, Bachvarova, RF *et al.* (1994). Expression of transcription factor HNF-4 in the extraembryonic endoderm, gut, and nephrogenic tissue of the developing mouse embryo: HNF-4 is a marker for primary endoderm in the implanting blastocyst. *Proc Natl Acad Sci USA* **91**: 7598–7602.
10. Taraviras, S, Monaghan, AP, Schütz, G and Kelsey, G (1994). Characterization of the mouse HNF-4 gene and its expression during mouse embryogenesis. *Mech Dev* **48**: 67–79.
11. Parviz, F, Matullo, C, Garrison, WD, Savatski, L, Adamson, JW, Ning, G *et al.* (2003). Hepatocyte nuclear factor 4alpha controls the development of a hepatic epithelium and liver morphogenesis. *Nat Genet* **34**: 292–296.
12. Odom, DT, Zizlsperger, N, Gordon, DB, Bell, GW, Rinaldi, NJ, Murray, HL *et al.* (2004). Control of pancreas and liver gene expression by HNF transcription factors. *Science* **303**: 1378–1381.
13. Battle, MA, Konopka, G, Parviz, F, Gaggl, AL, Yang, C, Sladek, FM *et al.* (2006). Hepatocyte nuclear factor 4alpha orchestrates expression of cell adhesion proteins during the epithelial transformation of the developing liver. *Proc Natl Acad Sci USA* **103**: 8419–8424.
14. Konopka, G, Tekiela, J, Iverson, M, Wells, C and Duncan, SA (2007). Junctional adhesion molecule-A is critical for the formation of pseudocanaliculi and modulates E-cadherin expression in hepatic cells. *J Biol Chem* **282**: 28137–28148.
15. Li, J, Ning, G and Duncan, SA (2000). Mammalian hepatocyte differentiation requires the transcription factor HNF-4alpha. *Genes Dev* **14**: 464–474.
16. Hayhurst, GP, Lee, YH, Lambert, G, Ward, JM and Gonzalez, FJ (2001). Hepatocyte nuclear factor 4alpha (nuclear receptor 2A1) is essential for maintenance of hepatic gene expression and lipid homeostasis. *Mol Cell Biol* **21**: 1393–1403.
17. Khurana, S, Jaiswal, AK and Mukhopadhyay, A (2010). Hepatocyte nuclear factor-4alpha induces transdifferentiation of hematopoietic cells into hepatocytes. *J Biol Chem* **285**: 4725–4731.
18. Suetsugu, A, Nagaki, M, Aoki, H, Motohashi, T, Kunisada, T and Moriwaki, H (2008). Differentiation of mouse hepatic progenitor cells induced by hepatocyte nuclear factor-4 and cell transplantation in mice with liver fibrosis. *Transplantation* **86**: 1178–1186.
19. Koizumi, N, Mizuguchi, H, Utoguchi, N, Watanabe, Y and Hayakawa, T (2003). Generation of fiber-modified adenovirus vectors containing heterologous peptides in both the HI loop and C terminus of the fiber knob. *J Gene Med* **5**: 267–276.
20. Shiojiri, N (1984). The origin of intrahepatic bile duct cells in the mouse. *J Embryol Exp Morphol* **79**: 25–39.
21. Moll, R, Franke, WW, Schiller, DL, Geiger, B and Krepler, R (1982). The catalog of human cytokeratins: patterns of expression in normal epithelia, tumors and cultured cells. *Cell* **31**: 11–24.

22. Antoniou, A, Raynaud, P, Cordi, S, Zong, Y, Tronche, F, Stanger, BZ *et al.* (2009). Intrahepatic bile ducts develop according to a new mode of tubulogenesis regulated by the transcription factor SOX9. *Gastroenterology* **136**: 2325–2333.
23. Offield, MF, Jetton, TL, Labosky, PA, Ray, M, Stein, RW, Magnuson, MA *et al.* (1996). PDX-1 is required for pancreatic outgrowth and differentiation of the rostral duodenum. *Development* **122**: 983–995.
24. Sussel, L, Kalamaras, J, Hartigan-O'Connor, DJ, Meneses, JJ, Pedersen, RA, Rubenstein, JL *et al.* (1998). Mice lacking the homeodomain transcription factor Nkx2.2 have diabetes due to arrested differentiation of pancreatic beta cells. *Development* **125**: 2213–2221.
25. Ingelman-Sundberg, M, Oscarson, M and McLellan, RA (1999). Polymorphic human cytochrome P450 enzymes: an opportunity for individualized drug treatment. *Trends Pharmacol Sci* **20**: 342–349.
26. Henderson, CJ, Otto, DM, Carrie, D, Magnuson, MA, McLaren, AW, Rosewell, I *et al.* (2003). Inactivation of the hepatic cytochrome P450 system by conditional deletion of hepatic cytochrome P450 reductase. *J Biol Chem* **278**: 13480–13486.
27. Yamada, T, Yoshikawa, M, Kanda, S, Kato, Y, Nakajima, Y, Ishizaka, S *et al.* (2002). *In vitro* differentiation of embryonic stem cells into hepatocyte-like cells identified by cellular uptake of indocyanine green. *Stem Cells* **20**: 146–154.
28. Anzenbacher, P and Anzenbacherová, E (2001). Cytochromes P450 and metabolism of xenobiotics. *Cell Mol Life Sci* **58**: 737–747.
29. Zhao, D, Chen, S, Cai, J, Guo, Y, Song, Z, Che, J *et al.* (2009). Derivation and characterization of hepatic progenitor cells from human embryonic stem cells. *PLoS ONE* **4**: e6468.
30. Hatta, K, Takagi, S, Fujisawa, H and Takeichi, M (1987). Spatial and temporal expression pattern of N-cadherin cell adhesion molecules correlated with morphogenetic processes of chicken embryos. *Dev Biol* **120**: 215–227.
31. Shiojiri, N (1981). Enzymo- and immunocytochemical analyses of the differentiation of liver cells in the prenatal mouse. *J Embryol Exp Morphol* **62**: 139–152.
32. Lee, JM, Dedhar, S, Kalluri, R and Thompson, EW (2006). The epithelial-mesenchymal transition: new insights in signaling, development, and disease. *J Cell Biol* **172**: 973–981.
33. Macleod, KF, Sherry, N, Hannon, G, Beach, D, Tokino, T, Kinzler, K *et al.* (1995). p53-dependent and independent expression of p21 during cell growth, differentiation, and DNA damage. *Genes Dev* **9**: 935–944.
34. Si-Tayeb, K, Noto, FK, Nagaoka, M, Li, J, Battle, MA, Duris, C *et al.* (2010). Highly efficient generation of human hepatocyte-like cells from induced pluripotent stem cells. *Hepatology* **51**: 297–305.
35. Sekiya, S and Suzuki, A (2011). Direct conversion of mouse fibroblasts to hepatocyte-like cells by defined factors. *Nature* **475**: 390–393.
36. Huang, P, He, Z, Ji, S, Sun, H, Xiang, D, Liu, C *et al.* (2011). Induction of functional hepatocyte-like cells from mouse fibroblasts by defined factors. *Nature* **475**: 386–389.
37. Satohisa, S, Chiba, H, Osanai, M, Ohno, S, Kojima, T, Saito, T *et al.* (2005). Behavior of tight-junction, adherens-junction and cell polarity proteins during HNF-4alpha-induced epithelial polarization. *Exp Cell Res* **310**: 66–78.
38. Xu, ZL, Mizuguchi, H, Sakurai, F, Koizumi, N, Hosono, T, Kawabata, K *et al.* (2005). Approaches to improving the kinetics of adenovirus-delivered genes and gene products. *Adv Drug Deliv Rev* **57**: 781–802.
39. Nagata, S, Toyoda, M, Yamaguchi, S, Hirano, K, Makino, H, Nishino, K *et al.* (2009). Efficient reprogramming of human and mouse primary extra-embryonic cells to pluripotent stem cells. *Genes Cells* **14**: 1395–1404.
40. Makino, H, Toyoda, M, Matsumoto, K, Saito, H, Nishino, K, Fukawatase, Y *et al.* (2009). Mesenchymal to embryonic incomplete transition of human cells by chimeric OCT4/3 (POU5F1) with physiological co-activator EWS. *Exp Cell Res* **315**: 2727–2740.
41. Furue, MK, Na, J, Jackson, JP, Okamoto, T, Jones, M, Baker, D *et al.* (2008). Heparin promotes the growth of human embryonic stem cells in a defined serum-free medium. *Proc Natl Acad Sci USA* **105**: 13409–13414.
42. Mizuguchi, H and Kay, MA (1998). Efficient construction of a recombinant adenovirus vector by an improved *in vitro* ligation method. *Hum Gene Ther* **9**: 2577–2583.
43. Mizuguchi, H and Kay, MA (1999). A simple method for constructing E1- and E1/E4-deleted recombinant adenoviral vectors. *Hum Gene Ther* **10**: 2013–2017.
44. Kawabata, K, Sakurai, F, Yamaguchi, T, Hayakawa, T and Mizuguchi, H (2005). Efficient gene transfer into mouse embryonic stem cells with adenovirus vectors. *Mol Ther* **12**: 547–554.
45. Tashiro, K, Kawabata, K, Sakurai, H, Kurachi, S, Sakurai, F, Yamanishi, K *et al.* (2008). Efficient adenovirus vector-mediated PPAR gamma gene transfer into mouse embryoid bodies promotes adipocyte differentiation. *J Gene Med* **10**: 498–507.
46. Maizel, JV Jr, White, DO and Scharff, MD (1968). The polypeptides of adenovirus. I. Evidence for multiple protein components in the virion and a comparison of types 2, 7A, and 12. *Virology* **36**: 115–125.
47. Smith, MT (2003). Mechanisms of troglitazone hepatotoxicity. *Chem Res Toxicol* **16**: 679–687.
48. Dai, Y and Cederbaum, AI (1995). Cytotoxicity of acetaminophen in human cytochrome P4502E1-transfected HepG2 cells. *J Pharmacol Exp Ther* **273**: 1497–1505.
49. Chang, TK, Weber, GF, Crespi, CL and Waxman, DJ (1993). Differential activation of cyclophosphamide and ifosphamide by cytochromes P-450 2B and 3A in human liver microsomes. *Cancer Res* **53**: 5629–5637.
50. Miao, XS and Metcalfe, CD (2003). Determination of carbamazepine and its metabolites in aqueous samples using liquid chromatography-electrospray tandem mass spectrometry. *Anal Chem* **75**: 3731–3738.

Analytical Biochemistry 421 (2012) 595–606

Contents lists available at SciVerse ScienceDirect

Analytical Biochemistry

journal homepage: www.elsevier.com/locate/yabio

One-pot characterization of cancer cells by the analysis of mucin-type glycans and glycosaminoglycans

Keita Yamada [a,b], Yosuke Mitsui [a], Naotaka Kakoi [a], Mitsuhiro Kinoshita [a], Takao Hayakawa [c], Kazuaki Kakehi [a,*]

[a] School of Pharmacy, Kinki University, Higashi-Osaka, Osaka 577-8502, Japan
[b] Division of Glyco-Bioindustry, Life Science Research Center, Institute of Research Promotion, Kagawa University, Miki-cho, Kita-gun, Kagawa 761-0793, Japan
[c] Pharmaceutical Research and Technology Institute, Kinki University, Higashi-Osaka, Osaka 577-8502, Japan

ARTICLE INFO

Article history:
Received 14 September 2011
Received in revised form 5 December 2011
Accepted 8 December 2011
Available online 14 December 2011

Keywords:
Mucin-type glycans
Glycosaminoglycans
Serotonin affinity chromatography
Capillary electrophoresis
MALDI–TOF MS
Cancer cells

ABSTRACT

We developed an automated apparatus for rapid releasing of *O*-glycans from mucin-type glycoproteins [Anal. Biochem. 371 (2007) 52–61; Anal. Chem. 82 (2010) 7436–7443] and applied the device to analyze them in some cancer cell lines [J. Proteome Res. 8 (2009) 521–537]. We also found that the device is useful to release glycosaminoglycans from proteoglycans [Anal. Biochem. 362 (2007) 245–251]. Based on these studies, we developed a method for one-pot analysis of mucin-type glycans and glycosaminoglycans after releasing them from total protein pool obtained from some cancer cell lines. Mucin-type glycans were analyzed by a combination of high-performance liquid chromatography and mass spectrometry techniques, and glycosaminoglycans were analyzed by capillary electrophoresis as fluorescent-labeled unsaturated disaccharides after digestion with specific eliminases followed by fluorescent labeling. Ten cancer cell lines, including blood cancer cells as well as epithelial cancer cells, were used to assess the method. The results clearly revealed that both mucin-type glycans and glycosaminoglycans showed quite interesting profiles. Thus, the current technique will be a powerful tool for discovery of glycan markers of diseases.

Analysis of glycan structures has become one of the requirements of postgenomic research. Most of the glycans attached to glycoproteins are classified into *N*- and *O*-glycans. Because of the extremely complex structures and heterogeneity of both *N*- and *O*-glycans, we often need to analyze their structures after releasing them from the core protein. In the analysis of *N*-glycans, *N*-glycoamidase having broad specificity is generally used to release *N*-glycans from the peptide backbone. We reported two methods for the analysis of *N*-glycans by labeling with 9-fluorenylmethyl chloroformate and 2-aminobenzoic acid (2AA)[1] [1,2]. These two methods allow sensitive analysis of *N*-glycans by high-performance liquid chromatography (HPLC), capillary electrophoresis (CE), and mass spectrometry (MS). We also achieved comprehensive analysis of *N*-glycans in various cancer cell lines and antibody pharmaceuticals [2,3].

In contrast, structural and quantitative analysis of *O*-glycans attached to the mucin-type glycoproteins has been a difficult task due to lack of appropriate *O*-glycan releasing methods. β-Elimination under mild alkaline conditions is still commonly employed but requires long reaction times. In addition, reducing reagents such as sodium borohydride need to be added to prevent unwanted degradation of the released glycans (i.e., peeling) [4–6]. This causes a loss of the original reducing terminal, and the released glycans do not have an aldehyde group, which is important for sensitive detection and high-resolution analysis by labeling with sensitive fluorescent or chromophoric reagents.

Release of *O*-glycans with the intact reducing end has been reported. Royle and coworkers employed mild hydrazinolysis to afford free *O*-glycans from microgram quantities of glycoproteins, but a lengthy reaction time and reacetylation of de-N-acetylated groups are required [7]. Huang and coworkers developed a method for releasing *O*-glycans in the presence of ammonia, but the method also requires a long reaction time [8].

Recently, we developed an automatic *O*-glycan releasing apparatus to obtain *O*-glycans from core proteins as free form. The apparatus enables release of *O*-glycans within only 3 min without significant degradations of the released glycans. In addition, our method showed excellent repeatability [9,10]. We also connected

* Corresponding author. Fax: +81 6 6721 2353.
E-mail address: k_kakehi@phar.kindai.ac.jp (K. Kakehi).

[1] *Abbreviations used:* 2AA, 2-aminobenzoic acid; HPLC, high-performance liquid chromatography; CE, capillary electrophoresis; MS, mass spectrometry; MALDI–TOF, matrix-assisted laser desorption/ionization time-of-flight; GAG, glycosaminoglycan; HS, heparan sulfate; HA, hyaluronic acid; DHB, 2,5-dihydroxybenzoic acid; $NaBH_4$, sodium borohydride; PBS, phosphate-buffered saline; MWCO, molecular weight cutoff; NP–HPLC, normal phase HPLC; MS/MS, tandem MS; CS, chondroitin sulfate.

0003-2697/$ - see front matter © 2011 Elsevier Inc. All rights reserved.
doi:10.1016/j.ab.2011.12.017

this system to an automatic spotter (AccuSpot from Shimadzu) for direct matrix-assisted laser desorption/ionization time-of-flight (MALDI–TOF) MS measurement for routine analysis of *O*-glycans, and the analysis of the released *O*-glycans is completed within 1.5 h [11].

During the releasing reaction, we found that glycosaminoglycans (GAGs) are also conveniently released from proteoglycans. The released GAGs are digested with specific eliminases to produce a mixture of unsaturated disaccharides that are conveniently labeled with a fluorescent tag such as 2AA or 2-aminoacridone and analyzed by CE [12].

These two types of *O*-glycans (mucin-type glycans and GAGs) are concerned with various biological functions [13–16], and there are a number of research works on the aberrant glycan patterns in relation to progression of diseases [17–20]. Structural alterations of mucin-type glycans are often observed in tumors. For example, core 3 and core 4 mucin-type glycans are synthesized in normal cells but apparently down-regulated in gastric and colorectal carcinoma [21,22] (see Supplementary Fig. 1 in supplementary material for the core structures of *O*-glycans). Iwai and coworkers showed that expression of the enzymes related to the synthesis of core 3 structure reduced tumor formation in human fibrosarcoma cells [22]. Cancer-associated mucin-type glycans were highly sialylated but less sulfated and were often truncated [23–25]. Truncated mucin-type glycans such as Tn and T antigens as well as their sialylated analogues became predominant with the progression of cancer [26]. The occurrence of the sialyl-Lewis^x (NeuAcα2-3Galβ1-4(Fucα1-3)GlcNAcβ1-3Gal-R:SLe^x) epitope on *O*-glycans in colon cancer patients is also associated with poor survival [27]. In addition, metastatic cancer cells often express the increased amounts of sialyl-Lewis^a epitope (NeuAcα2-3Galβ1-3(Fucα1-4)GlcNAcβ1-3Gal-R:SLe^a) and SLe^x [28,29].

Many reports on the alterations of GAGs in relation to tumorigenesis have also appeared. Nonsulfated chondroitin is detected in tumor tissues, whereas it is almost absent in normal specimens [30]. Furthermore, differences in the sulfation pattern of heparan sulfate (HS) were also reported [31]. For example, HS from lung cancer cells exhibited a higher degree of oversulfation that was due to an increased content of the three repeating disaccharides having 6-*O*-sulfated glucosamine residues [31]. Highly sulfated HS acts as a coreceptor for a variety of pro-angiogenic factors, such as vascular endothelial growth factor and fibroblast growth factor, and plays vital roles throughout the various stages of angiogenesis and tumor growth [32–34]. Increased levels of hyaluronic acid (HA) are also associated with certain types of human primary and metastatic cancers [35,36]. Vizoso and coworkers measured the expression level of HA in gastric tumor tissues from 129 patients, and they revealed that high expression of HA is an indicator of poor prognosis for patients with gastric cancer [37].

Glycans are not the direct products by genes; rather, they are the product by a combination of actions of the relevant enzymes. Therefore, alteration of structure simultaneously occurs in some glycans, and comprehensive analysis of glycan structures is required to reveal the relationship between biological characteristics and glycans. Two types of these *O*-glycans described above were commonly attached to serine (or threonine) residues on peptides and can be affected with each other. Based on these considerations, determination of alterations of multiple kinds of glycans will lead to accurate understanding of diseases, including tumors.

Unfortunately, it should be noticed that profiles of mucin-type *O*-glycans and GAGs have been reported independently. In addition, there is little information on the relationship between the changes of mucin-type *O*-glycans and GAGs. If we can obtain both types of information at the same time, the amount of knowledge on both glycans can increase dramatically and will be an important tool for cancer diagnostics and therapies. Based on these considerations, this study aimed at one-pot analysis of mucin-type *O*-glycans and GAGs.

Materials and methods

Materials

Pronase (*Streptomyces griseus*) was obtained from Calbiochem (San Diego, CA, USA). 2AA and sodium cyanoborohydride for fluorescent labeling of the released glycans were obtained from Tokyo Kasei (Tokyo, Japan) and Sigma–Aldrich Japan (Tokyo, Japan), respectively. Sephadex LH-20 was obtained from GE Healthcare (Tokyo, Japan). Triton X-100, 2,5-dihydroxybenzoic acid (DHB), and sodium borohydride ($NaBH_4$) were also obtained from Sigma–Aldrich Japan. Protein inhibitor cocktail for animal cells was obtained from Nacalai Tesque (Kyoto, Japan). A serotonin-immobilized column for the separation of sialo glycans was obtained from Seikagaku Biobusiness (Tokyo, Japan). Chondroitinase ABC, heparitinase 1, heparitinase 2, and standard samples of unsaturated disaccharides for the analysis of GAGs were also obtained from Seikagaku Biobusiness. Fused silica capillary tubing (50 μm i.d.) was obtained from GE Healthcare. Other reagents and solvents were of the highest grade commercially available or HPLC grade. All aqueous solutions were prepared using water purified with a Milli-Q purification system (Millipore, Bedford, MA, USA).

Cell cultures

In the current study, human-derived cancer cells were employed: U937 (histiocytic lymphoma), K562 (chronic myelogenous leukemia), Jurkat (acute T cell leukemia), HL-60 (acute promyelocytic leukemia), LS174T (colorectal adenocarcinoma), HCT116 (colorectal adenocarcinoma), HCT15 (colorectal adenocarcinoma), BxPC3 (pancreatic adenocarcinoma), PANC1 (pancreatic carcinoma), and MKN7 and MKN45 (gastric adenocarcinoma). All of these cells except LS174T were cultured in RPMI 1640 medium supplemented with 10% (v/v) fetal calf serum and 1% (v/v) penicillin/streptomycin mixed solution (10,000 U/ml penicillin and 10 mg/ml streptomycin, Nacalai Tesque). LS174T cells were cultured in minimum essential medium supplemented with 10% (v/v) fetal calf serum. Fetal calf serum was previously kept at 56 °C for 30 min. The cells were cultured at 37 °C under 5% CO_2 atmosphere and harvested at 80% confluent state. Collected cells (1.0×10^7 cells) were washed with phosphate-buffered saline (PBS) and collected by centrifugation at 1000 rpm for 20 min.

Glycopeptide pool from whole cells

Glycopeptide pool derived from cancer cells was prepared according to the method reported previously [38]. Cultured cells (1.0×10^7 cells) were suspended in 5 mM Tris–HCl buffer (pH 8.0, 500 μl) and mixed with an equal volume of 2% Triton X-100 in the same buffer in an ice bath. After homogenizing the cells for 7 min with a glass homogenizer, the mixture was centrifuged at 8000*g* for 30 min. The supernatant layer was collected and boiled for 7 min at 100 °C and evaporated to dryness by a centrifugal evaporator (SpeedVac, Savant, Sunnydale, CA, USA). The lyophilized material was suspended in water (200 μl), and ethanol (800 μl) was added to the mixture to 80% concentration. The precipitate was collected by centrifugation and washed with ethanol (1 ml × 3) and then with acetone (1 ml × 2), followed by drying in vacuo. The residue was digested with pronase (50 μg) in 50 mM Tris–HCl (pH 8.0, 200 μl) at 37 °C for 24 h. The reaction mixture was boiled for 10 min, and the supernatant was collected after centrifugation. Because free glycans present in some cancer cells inhibit the subsequent analysis of *O*-glycans [39], reduction

with $NaBH_4$ prior to *O*-glycan releasing reaction is necessary. An aqueous solution of 2 M $NaBH_4$ (500 μl) was added to the supernatant and kept at room temperature for 30 min. Glacial acetic acid was carefully added to the mixture to decompose excess $NaBH_4$, and the mixture was passed through an ultrafiltration membrane (5000 MWCO [molecular weight cutoff], Amicon Ultra, Millipore) at 10,000*g*. The mixture of glycopeptides on the membrane was dissolved in water (100 μl) and used for releasing reaction of *O*-glycans from mucin-type glycoproteins and proteoglycans.

Releasing reactions of O-glycans

Releasing reaction of *O*-glycans using the automated glycan releasing system was performed according to the method reported previously [9]. Briefly, an aqueous solution of 0.5 M LiOH was used as the releasing reagent and the eluent. To the flow of the eluent at 1.0 ml/min, an aqueous solution of the mixture of glycopeptides from each cell line (5.0×10^6 cells/50 μl) obtained as described above was injected. After the sample solution was mixed with the eluent in the mixing device, the mixed solution was moved to the reactor kept at 60 °C, in which a reaction tube (0.25 mm i.d., 10 m length, 700 μl volume) was set. During passing through the reaction tube in the reactor, *O*-glycans were released from the peptide. The eluate containing the reaction mixture from the reactor was immediately introduced to a cartridge (1.0 ml volume) packed with cation exchange resin and collected to a fraction collector installed in the system while monitoring the absorbance at 230 nm. The collected solution containing the released *O*-glycans was evaporated to dryness by a centrifugal evaporator, and the dried material was used for fluorescent labeling with 2AA.

Fluorescent labeling of the released O-glycans with 2AA

The mixture of the released *O*-glycans was dissolved in 2AA solution (200 μl), which was freshly prepared by dissolution of 2AA (30 mg) and sodium cyanoborohydride (30 mg) in methanol (1 ml) containing 4% sodium acetate and 2% boric acid. The mixture was kept at 80 °C for 1 h. After cooling, water (100 μl) was added and the mixture was applied to a column of Sephadex LH-20 (1.0 cm i.d., 30 cm length) previously equilibrated with 50% aqueous methanol. The earlier eluted fluorescent fractions were pooled and evaporated to dryness under reduced pressure. The dried residue was dissolved in water (40 μl), and a portion (20 μl) was injected to analyze by serotonin affinity chromatography.

Serotonin affinity chromatography for separation of O-glycans and GAGs

Mucin-type glycans and GAGs are analyzed according to the procedures (see Supplementary Fig. 2 in supplementary material). Serotonin affinity chromatography for group separation of glycans based on the number of attached sialic acid residues was performed with a Jasco HPLC apparatus equipped with two PU-980 pumps and a Jasco FP-920 fluorescence detector (Tokyo, Japan) using a serotonin-immobilized column (4.6 × 150 mm) with linear gradient from water (solvent A) to 50 mM ammonium acetate (solvent B) at a flow rate of 0.5 ml/min. Initially solvent B was used at 5% concentration for 2 min, and then linear gradient elution was performed to 37% B for 16 min. After collecting mucin-type glycans, an aqueous solution of 1 M NaCl was used to elute GAGs during the subsequent 15 min. The column was then equilibrated with the starting eluent. After group separation, mucin-type glycan fractions were analyzed by MALDI–TOF MS and normal phase HPLC (NP–HPLC). In addition, GAG fractions were digested with specific eliminases and analyzed by CE after labeling with 2AA.

HPLC analysis of mucin-type glycans

The apparatus was the same as described above. Separation was done with a TSK-GEL Amide-80 column (Tosoh, 4.6 × 250 mm) using a linear gradient formed by 0.1% acetic acid in acetonitrile (solvent A) and 0.2% acetic acid in water containing 0.1% triethylamine (solvent B) at 40 °C. The column was initially equilibrated and eluted with 85% solvent A for 2 min, from which point solvent B was increased to 50% over 80 min at 1.0 ml/min. Then, the column was washed with 90% B for 10 min and equilibrated at initial conditions for 15 min. The amounts of mucin-type glycans were calculated from the peak areas based on the standard curve prepared using maltopentaose labeled with 2AA.

MALDI–TOF MS analysis of mucin-type glycans separated by serotonin affinity chromatography

MALDI–TOF MS spectra of 2AA-labeled glycans were acquired on a Voyager-DE Pro mass spectrometer (PE Biosystems, Framingham, MA, USA) in negative or positive ion linear mode with a nitrogen laser (338 nm) for the ionization source. Accelerating voltage was set at 20 kV, and delayed extraction was performed after 800 ns. DHB was used as matrix material throughout the work. The mass numbers of the molecular ion peaks were corrected using a mixture of 2AA-labeled dextran oligomers as standard mass markers. The sample solution (1 μl) was mixed with 2% DHB (1 μl) in ethanol on a stainless-steel plate, and the mixture was dried under atmosphere at room temperature.

MS^n analysis of mucin-type glycans

Structures of mucin-type glycans were confirmed by the MS^n technique on a MALDI–quadrupole ion trap–TOF mass spectrometer (AXIMA-Resonance, Shimadzu, Kyoto, Japan). Acquisition and data processing were controlled by Launchpad software (Kratos Analytical, Manchester, UK). For collision-induced dissociation, argon was used as the collision gas. For the sample preparation, a 0.5-μl volume of the matrix solution (DHB, 10 mg/ml in 30% ethanol) was deposited on the stainless-steel target plate and allowed to dry. Then, a portion (0.5 μl) of the appropriately diluted analyte solution (typically ~1 pmol/μl) was applied to cover the matrix on the target plate and allowed to dry.

Analysis of GAGs collected by serotonin affinity chromatography

After collecting the GAG pool by serotonin affinity chromatography, the GAG pool was passed through a filter device (3000 MWCO). Half of the GAG mixture on the membrane was dissolved in 50 mM Tris–HCl buffer (pH 8.0, 100 μl). Chondroitinase ABC (0.5 U) dissolved in the same buffer (10 μl) was added to the solution and kept at 37 °C overnight. The other half of the GAG mixture was dissolved in 100 mM sodium acetate/0.1 mM calcium acetate (pH 7.0, 100 μl). Heparitinases 1 and 2 (5 mU/10 μl each) were added to the solution, and the mixture was kept at 37 °C overnight. Both reaction mixtures obtained by digestion with chondroitinase ABC and heparitinases were labeled with 2AA and analyzed by CE.

CE analysis of unsaturated disaccharides from GAGs

CE was performed on a P/ACE MDQ Glycoprotein System (Beckman Coulter, Fullerton, CA, USA) equipped with a helium–cadmium laser-induced fluorescence detector (excitation 325 nm, emission 405 nm). For the analysis of 2AA-labeled unsaturated disaccharides derived from GAGs, electrophoresis was performed with a fused silica capillary (50 μm i.d. × 30 cm) in 100 mM Tris–phosphate buffer (pH 3.0). Sample solutions were introduced into

the capillary by pressure injection at 1 psi for 10 s. Separation was performed by applying the potential of 25 kV at 25 °C.

The amounts of unsaturated disaccharides were calculated from the peak areas based on the standard curve prepared using standard samples of unsaturated disaccharides labeled with 2AA.

Results and discussion

Separation of mucin-type glycans and GAGs by serotonin affinity chromatography

We have been employing serotonin affinity chromatography for group separation of 2AA-labeled *N*- and mucin-type glycans prepared from various cancer cell lines using gradient elution with ammonium acetate. The separation is achieved based on the number of sialic acid residues [2,38], and the glycans separated in this way are analyzed by HPLC and MS without further purification steps because the glycan fractions are in an aqueous solution of volatile salts at low concentrations. This is one of the advantages of serotonin affinity chromatography.

During the studies on the analysis of the released glycans, we found that GAGs are also retarded on a serotonin-immobilized column (Fig. 1). An example for the analysis of oligomers derived from hyaluronan (HA oligomers) is shown in Fig. 1A. HA oligomers were strongly retained on the serotonin-immobilized stationary phase based on their total negative charges (i.e., oligomers having the higher molecular weight are eluted later). It is considered that glucuronic acid residues in HA molecules play important roles in interaction with serotonin. We also analyzed the artificial mixture of mucin-type glycans from fetuin and HA oligomers (Fig. 1B). Mucin-type glycans from fetuin were observed at 8 and 15 min, and then HA oligomers were observed. The results indicated that serotonin affinity chromatography is useful for group separation of mucin-type glycans and GAGs. Based on these results, we developed the procedures for one-pot analysis of mucin-type glycans and GAGs as described in Materials and methods and applied the method to the analysis of *O*-glycans on HCT116 cells (colorectal adenocarcinoma).

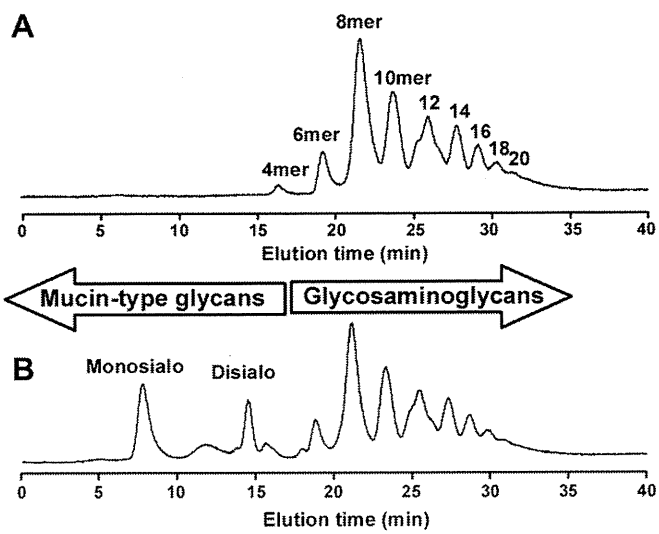

Fig.1. Separation of mucin-type glycans and GAGs by serotonin affinity chromatography. 2AA-labeled HA oligosaccharides (A) and a mixture of HA oligosaccharides and mucin-type glycans derived from bovine fetuin (B) are shown. Analytical conditions: eluent, water (solvent A) and 40 mM ammonium acetate (solvent B); gradient condition, linear gradient (5–75% solvent B) from 2 to 37 min and 75 to 100% solvent B from 37 to 45 min.

One-pot analysis of mucin-type glycans and GAGs from HCT116 cells

In the initial step of the analysis of *O*-glycans expressed on HCT116 cells, the released glycans were separated by serotonin affinity chromatography (Fig. 2). Asialo (M1), monosialo (M2 and M3) and disialo (M4–M6) mucin-type glycans were observed at 3–5, 5.2–10.0, and 10.8–16.0 min, respectively. After all mucin-type glycans were eluted, GAGs were eluted with 1 M NaCl. Each fraction obtained in this way was analyzed according to the method described in Materials and methods.

Six mucin-type glycan fractions (M1–M6) were analyzed by NP–HPLC and MALDI–TOF MS (Fig. 3), and the list of the observed mucin-type glycans in HCT116 cells is summarized in Table 1. The MS data were analyzed by Glycopeakfinder and Glycoworkbench in EUROCarbDB (http://www.ebi.ac.uk/eurocarb/tools.action). The amounts of expressed mucin-type glycans were calculated from the peak areas observed by NP–HPLC. We found 31 mucin-type glycans in HCT116 cells. Asialo glycans, T antigen (*m/z* 503: Galβ1-3GalNAc-2AA), core 2 structure (*m/z* 706: Galβ1-3(GlcNAcβ1-6)GalNAc-2AA), galactosyl core 2 structure (*m/z* 868: Galβ1-3(Galβ1-4GlcNAcβ1-6)GalNAc-2AA), and a polylactosamine-type glycan (*m/z* 1233: $Hex_3HexNAc_3$-2AA) were observed. Tandem MS (MS/MS) analysis of the peak observed at 1233 gave the ions at *m/z* 544 and 503 (Fig. 4A). These ions are obviously due to GlcNAcβ1-6GalNAc-2AA and Galβ1-3GalNAc-2AA (Fig. 4A). Based on these results, the glycan observed at *m/z* 1233 was confirmed as polylactosaminyl core 2 structure, Gal-GlcNAc-Galβ1-4 GlcNAcβ1-6(Galβ1-3)GalNAc-2AA. Monosialo core 1 and core 2 structures were found in monosialo glycan fractions (M2 and M3). Monosialo-polylactosamine-type glycans were also clearly observed in M2. These glycans have polylactosaminyl core 2 structure. Monosialo glycans having smaller molecular sizes such as sialyl-T and monosialo core 2 structure were observed in M3. Disialo core 1, core 2, and disialo-polylactosaminyl glycans were observed in M4, M5, and M6. It should be noted that mono sulfated mucin-type glycans were observed in HCT116 cells. The molecular ion at *m/z* 1604 observed in M6 is due to $NeuAc_1Hex_3HexNAc_3$-2AA + SO_3. After neuraminidase digestion, MS/MS analysis of this glycan afforded a desulfated molecular ion peak at *m/z* 1233 (Fig. 4B, upper spectrum). By MS^3 analysis, the fragment ion peak observed at *m/z* 1233 is confirmed as polylactosaminyl core 2 structure, Gal-GlcNAc-Galβ1–4 GlcNAcβ1-6(Galβ1-3)GalNAc-2AA (Fig. 4B, lower spectrum). In addition, two fragment ion peaks at *m/z* 444 and 948 were observed in MS^2 spectrum (Fig. 4B, upper spectrum). The fragment ion peak at *m/z* 444 corresponds to sulfated lactosamine, GalGlcNAc + SO_3. The fragment ion peak at *m/z*

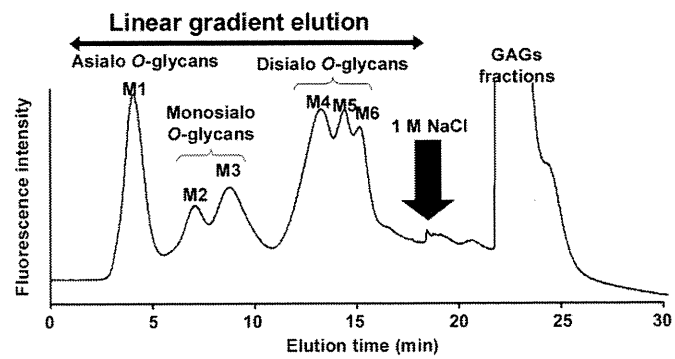

Fig.2. Separation of mucin-type glycans and GAGs derived from HCT116 cells by serotonin affinity chromatography. Analytical conditions: eluent, water (solvent A) and 40 mM ammonium acetate (solvent B); gradient condition, linear gradient (5–41% solvent B) from 2 to 20 min. After collecting the mucin-type glycans, GAGs were eluted with 1 M NaCl.

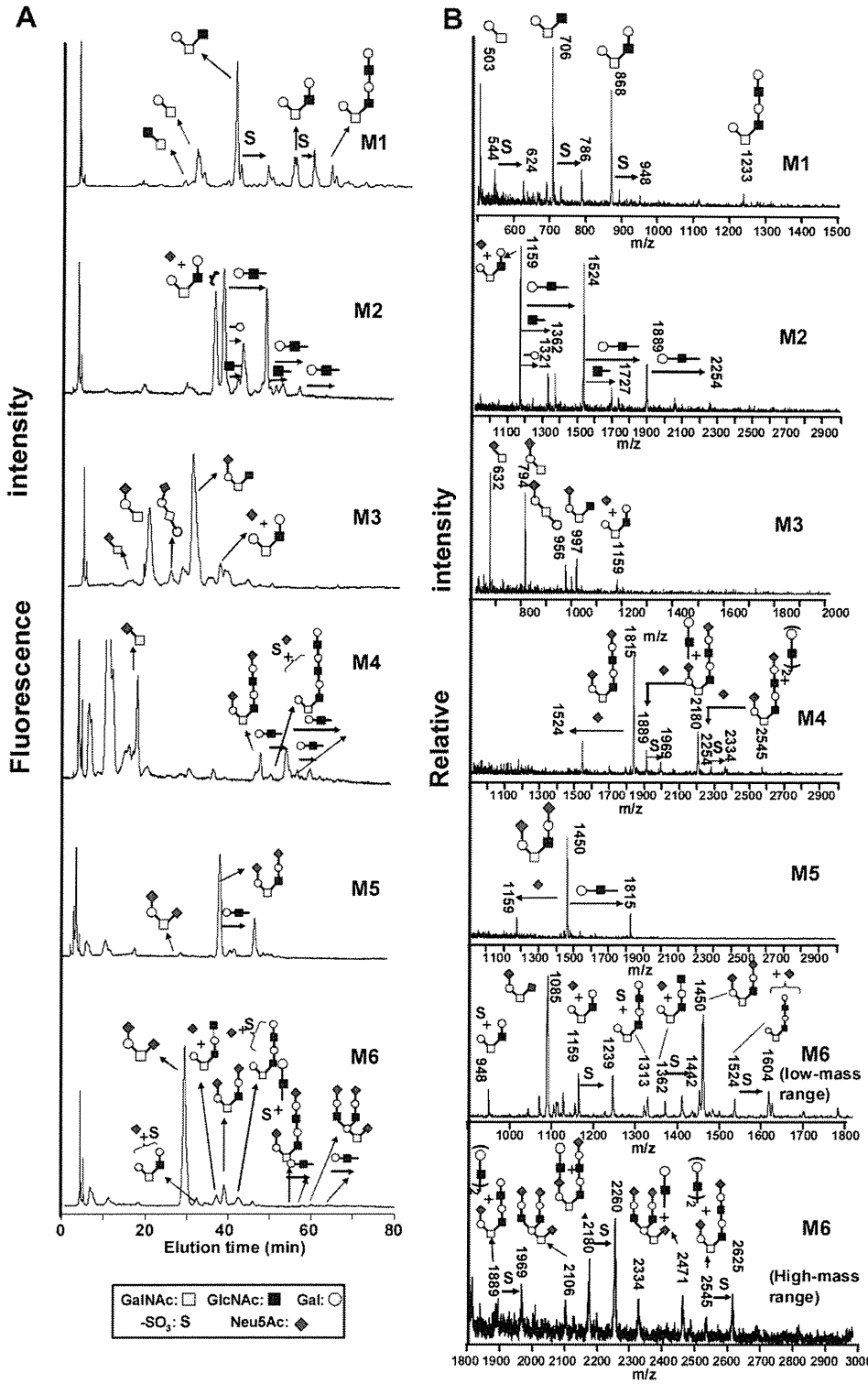

Fig.3. NP-HPLC and MALDI-TOF MS analysis of mucin-type glycans derived from HCT116 cells. The mucin-type glycan fractions separated by serotonin affinity chromatography were analyzed by NP-HPLC (A) and MALDI-TOF MS (B). Analytical conditions of HPLC: column, Amide-80 (Tosoh, 4.6 × 250 nm); solvent A, 0.1% CH_3COOH in acetonitrile; solvent B, 0.2% CH_3COOH–0.1% triethylamine in water; gradient condition, linear gradient (15–65% solvent B) from 2 to 82 min.

948 is due to sulfated galactosyl core 2 structure, Galβ1-4GlcNAcβ1-6(Galβ1-3)GalNAc-2AA + SO_3. This fragment ion indicates that terminal lactosamine is not sulfated. It was reported that GlcNAc-6-*O*-sulfotransferase was expressed and Gal-3-*O*-sulfotransferase was down-regulated in colon cancer cells [40]. Based on these considerations, we concluded that the structure of this sulfate-containing mucin-type glycan was Gal-GlcNAc-Galβ1-4(SO_3-6)GlcNAcβ1-6(Galβ1-3)GalNAc-2AA. These types of sulfated glycans were also observed in M1 and M4.

GAG fractions collected by serotonin affinity chromatography were analyzed as unsaturated disaccharides after digestion with specific eliminases. Half of the fractions were digested with chondroitinase ABC, and the other half were treated with a combination of heparitinases 1 and 2. The mixture of unsaturated disaccharides

Table 1
Mucin-type glycans found in HCT116 cells.

Structure	Observed molecular ion peaks (*m*/*z*)	Amount of glycans (pmol/L × 10^6 cells)
Asialo glycans		
Galβ1-3GalNAc-2AA	503	67.1
GlcNAcβ1-3GalNAc-2AA	544	0.5
Galβ1-3(GlcNAcβ1-6)GalNAc-2AA	706	142.1
Galβ1-3(Galβ1-4GlcNAcβ1-6)GalNAc-2AA	868	73.9
Galβ1-3(Gal-GlcNAc-Galβ1-4GlcNAcβ1-6)GalNAc-2AA	1233	41.8
Monosialo glycans		
NeuAcα2-6GalNAc-2AA	632	122.8
NeuAcα2-3Galβ1-3GalNAc-2AA	794	180.0
NeuAcα2-3Galβ1-3(GlcNAcβ1-6)GalNAc-2AA	997	294.3
Galβ1-3(Galβ1-4GlcNAcβ1-6)GalNAc-2AA + $NeuAc_1$	1159	191.7
Galβ1-3(GlcNAc-Galβ1-4GlcNAcβ1-6)GalNAc-2AA + $NeuAc_1$	1362	32.5
Galβ1-3(Gal-GlcNAc-Galβ1-4GlcNAcβ1-6)GalNAc-2AA + $NeuAc_1$	1524	120.7
Galβ1-3(GlcNAc-Gal-GlcNAc-Galβ1-4GlcNAcβ1-6)GalNAc-2AA + $NeuAc_1$	1727	34.3
Galβ1-3((Gal-GlcNAc)$_2$-Galβ1-4GlcNAcβ1-6)GalNAc-2AA + $NeuAc_1$	1889	32.8
Galβ1-3((Gal-GlcNAc)$_3$-Galβ1-4GlcNAcβ1-6)GalNAc-2AA + $NeuAc_1$	2254	21.5
Disialo glycans		
NeuAcα2-3Galβ1-3(NeuAcα2-6)GalNAc-2AA	1085	217.3
NeuAc-Galβ1-3(NeuAc-Galβ1-4GlcNAcβ1-6)GalNAc-2AA	1450	199.6
NeuAcα2-3Galβ1-3(NeuAc-Gal-GlcNAc-Galβ1-4GlcNAcβ1-6)GalNAc-2AA	1815	170.1
NeuAcα2-3Galβ1-3(NeuAc-(Gal-GlcNAc)$_2$-Galβ1-4GlcNAcβ1-6)GalNAc-2AA	2180	56.0
NeuAcα2-3Galβ1-3(NeuAc-(Gal-GlcNAc)$_3$-Galβ1-4GlcNAcβ1-6)GalNAc-2AA	2545	18.0
Trisialo glycans		
NeuAc-Gal-GlcNAc-(NeuAc-Gal-GlcNAc)Galβ1-3(NeuAcα2-6)GalNAc-2AA	2106	0.5
NeuAc-Gal-GlcNAc(NeuAc-Gal-GlcNAc)Galβ1-3(NeuAcα2-6)GalNAc-2AA + Gal-GlcNAc	2471	0.2
Sulfate glycans		
HexNAc-HexNAc-2AA + SO_3	624	2.3
Galβ1-3(GlcNAcβ1-6)GalNAc-2AA + SO_3	786	66.6
Galβ1-3(Galβ1-4GlcNAcβ1-6)GalNAc-2AA + SO_3	948	81.0
Galβ1-3(Galβ1-4GlcNAcβ1-6)GalNAc-2AA + NeuAc + SO_3	1239	8.8
Galβ1-3(GlcNAc-Galβ1-4GlcNAcβ1-6)GalNAc-2AA + NeuAc + SO_3	1442	17.7
Galβ1-3(Gal-GlcNAc-Galβ1-4GlcNAcβ1-6)GalNAc-2AA + $NeuAc_1$ + SO_3	1604	19.5
Galβ1-3((Gal-GlcNAc)$_2$-Galβ1-4GlcNAcβ1-6)GalNAc-2AA + $NeuAc_1$ + SO_3	1969	1.4
NeuAcα2-3Galβ1-3(NeuAc-(Gal-GlcNAc)$_2$-Galβ1-4GlcNAcβ1-6)GalNAc-2AA + SO_3	2260	3.2
Galβ1-3((Gal-GlcNAc)$_3$-Galβ1-4GlcNAcβ1-6)GalNAc-2AA + $NeuAc_1$ + SO_3	2334	0.2
NeuAcα2-3Galβ1-3(NeuAc-(Gal-GlcNAc)$_3$-Galβ1-4GlcNAcβ1-6)GalNAc-2AA + SO_3	2625	0.5

obtained in this way was labeled with 2AA and analyzed by laser-induced fluorescence (LIF)–CE (Fig. 5). Peaks were assigned by comparing the migration times with those of the standard unsaturated disaccharides. As shown in Fig. 5A (upper panel), we achieved excellent separation of nine unsaturated disaccharides from chondroitin sulfate (CS) and HA. We also succeeded in separation of seven unsaturated disaccharides from HS (Fig. 5B, upper panel). Five unsaturated disaccharides, ΔdiCS-diS_E (SE), ΔdiCS-6S (6S), ΔdiCS-4S (4S), ΔdiCS-0S (0S), and Δdi-HA (HA), were observed in the mixture after digestion with chondroitinase ABC (Fig. 5A, lower panel; see the list of the structures in Fig. 5A). Relative abundance of Δdi-HA was much higher than those of other unsaturated disaccharides in HCT116 cells. Seven unsaturated disaccharides, ΔdiHS-triS (TriS), ΔdiHS-diS3 (S3), ΔdiHS-diS2 (S2), ΔdiHS-diS1 (S1), ΔdiHS-6S (6S), ΔdiHS-NS (NS), and ΔdiHS-0S (0S), were observed in the mixture digested with a combination of heparitinases 1 and 2 (Fig. 5B, lower panel). Relative abundance of unsulfated HS disaccharide (HS0S) was much higher than those of other unsaturated disaccharides in HCT116 cells. It should be noted that there are no other contaminating peaks due to mucin-type *O*-glycans. From these results, it was revealed that mucin-type glycans as well as GAGs were able to be analyzed in the same sample.

Characterization of cancer cell lines

Based on the results obtained by the analysis of both mucin-type glycans and GAGs in HCT116 cells, we applied the methods to the analysis of both glycans on various cancer cells. The results are summarized in Figs. 6–8. Fig. 6 shows the total amount of mucin-type glycans and GAGs expressed on 10 cancer cell lines. The amounts of the expressed mucin-type glycans and GAGs were calculated from the peak areas observed by NP–HPLC and CE, respectively. There are significant differences in the expression levels of mucin-type glycans and GAGs among leukemia cells and epithelial cells. All leukemia cell lines poorly express both mucin-type glycans and GAGs. In contrast, epithelial cells express large amounts of them, although the amounts of the glycans are conspicuously varied among cell lines. There are 10–100 times larger amounts of mucin-type glycans than GAGs present on cancer cells. This is probably because proteoglycans are not present as conjugates in cell membrane but rather loosely interact with the components of cell surface. During the purification step of whole proteins, some portions of proteoglycans are not collected or the expression level of proteoglycans may be intrinsically lower than that of mucin-type glycans, although further studies are required. In any case, the data indicate that glycans are not dense on the floating blood cells. In contrast, glycans in epithelial cells, which form tumor tissues, are present in high density and seem to show important roles in exchanging intercellular information.

Figs. 7 and 8 show comparisons of relative abundances of mucin-type glycans and unsaturated disaccharides derived from glycosaminoglycans in cancer cells. Fig. 7 shows the glycan profiles obtained from four leukemia cells. All cell lines commonly contained sialyl-T and disialyl-T antigens as major mucin-type glycans. K562 and U937 cells especially contained these two glycans as the major glycans. Although it was difficult to discriminate these two cells only by mucin-type glycan analysis, profiling of GAGs